CHEMICAL REVIEWS

Volume 97, Number 1 January/February 1997

Synthetic Water-Oxidation Catalysts for Artificial Photosynthetic Water Oxidation†

Wolfgang Rüttinger and G. Charles Dismukes*

Princeton University, Hoyt Laboratory, Department of Chemistry, Princeton, New Jersey 08544

Received April 5, 1996 (Revised Manuscript Received October 2, 1996)

Contents

I. Introduction

Green plants, algae, and some cyanobacteria produce dioxygen by using water as the electron source for the production of reducing equivalents (NAPDH) and ATP during photosynthesis. This process coincided with the appearance of oxygen-dependent forms of life on earth, sustains the earth's atmosphere in its present constitution, and provides dioxygen as a metabolic oxidant. The four-electron oxidation of water in photosynthetic organisms is achieved by an inorganic cofactor bound to polypeptides of photosystem II (PSII) called the water-oxidizing complex (WOC). The mechanism of water oxidation at the molecular level by the WOC remains largely an unsolved mystery. Model complexes have played an indispensable role in our present understanding of the WOC, even though well-characterized functional models are rare. Water-oxidation catalysts are intrinsically important in their own right, independent of possible biological relevance. They have direct applications as catalysts in artificial photosynthetic systems for the splitting of water that could be used in future fuel cells for the generation of electricity. Such systems are commercially appealing in view of the decreasing energy resources and the environmental problems arising from combustion of coal, oil, and gas in air.

† List of abbreviations: NADPH, nicotineamide adenine dinucleotide phosphate; ATP, adenine triphosphate; WOC, water-oxidizing complex; PSII, photosystem II; bpy, 2,2′-bipyridine; py, pyridine; BPG, basal plane graphite; XAS, X-ray absorption spectroscopy; EXAFS, extended X-ray absorption fine structure; XANES, X-ray absorption near edge structure; EPR, electron paramagnetic resonance; ENDOR, electron nuclear double resonance; TON, turnover number.

S0009-2665(95)00201-9 CCC: $28.00

G. Charles Dismukes is Professor of Chemistry at Princeton University where he has been a member of the faculty since 1978. He received his Ph.D. in physical chemistry for research supervised by John Willard in the field of radiation chemistry at the University of Wisconsin in Madison and did postdoctoral research with Kenneth Sauer and Melvin Klein in the field of photobiology at the University of California in Berkeley. He was a visiting scholar at the Service de Biophysique of the Centre d-Etude Nucleares-Saclay in 1984 and at the Squibb Pharmaceutical Research Institute in 1991. He has received the Searle Scholars Award, 1981–1983, Alfred P. Sloane Award, 1984–1986, and a Japan Society for the Promotion of Science Award, 1992. His current research interests include structure and mechanisms of multimetal-containing enzymes and bioinspired inorganic catalysts.

Wolfgang Rüttinger is currently working on his Ph.D. in bioinorganic chemistry at Princeton University in the research group of Professor G. C. Dismukes, focusing on model complexes for the water-oxidizing complex of photosystem II. He previously received a masters (Diplom) degree at the University of Erlangen-Nürnberg in Germany working on carbon dioxide photoreduction on semiconductor powders.

This review focuses primarily on homogeneous catalysts for the oxidation of water, but does include selected heterogeneous systems. It does not attempt to summarize all chemistry related to systems that are capable of oxidizing water. In particular, heterogeneous catalysts that have no direct relevance to understanding the WOC are not discussed in detail. Neither are nonbiomimetic systems for artificial photosynthesis or water-splitting in its elements discussed. However, a list of some of the recent references in these areas can be found in section X (Nonbiomimetic Water Oxidation Catalysts).

We will first give a brief summary of the current view of the photosynthetic WOC and its functionality, followed by analysis of the thermodynamic and kinetic constraints for water-oxidation that have to be overcome by any catalyst. Since manganese is the metal that performs this reaction in the WOC, manganese catalysts will be discussed first, followed by other transition metals, particularly ruthenium. In the final section we summarize the principles of reactivity learned from theory and existing models that will guide us toward synthesis of better catalysts in the future. This review does not attempt to summarize manganese chemistry relevant to nonfunctional (structural) models of the WOC, which has been reviewed recently.[26,27]

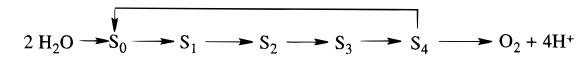

Figure 1. "Kok cycle" of water oxidation by PSII: S_i denotes the different oxidized states of the WOC that are generated by a train of light flashes prior to the generation of oxygen.

II. Structural and Mechanistic Constraints on Photosynthetic Water Oxidation

A. Overview

According to present knowledge, all species which produce dioxygen during photosynthesis possess qualitatively the same WOC, comprised of four manganese ions, one or two calcium ion(s), and an unspecified number of chloride ions.[28] The four manganese ions exist as an electronically coupled tetramer which is the site of water oxidation. No other metal has been found to replace it, neither *in vivo* nor by reconstitution of manganese-depleted samples. Calcium appears to play a structural role in stabilizing the Mn site and possibly as a gatekeeper in restricting access of substrate water to the Mn site.[29] Calcium can be substituted by strontium, yielding a 40% lower O_2 evolution activity.[30] Chloride has been proposed to serve as a labile ligand to the Mn site, where it might block premature substrate oxidation, as a nonlabile ligand to Mn functioning to set the redox potential of the cluster, and possibly as a bridging ligand between Mn ions, where it might promote intracluster electron transfer. Chloride can be replaced by bromide and a few other anions but always with lower O_2 evolution rates.[28,31]

A key advance in our understanding of the functional organization of the WOC was the work by Joliot and Kok and their co-workers.[32] Illumination of dark-adapted spinach chloroplasts by short flashes of light led to a characteristic pattern of O_2 release, repeating after each four flashes. This led to the formulation of what is known as the Kok cycle of water oxidation (Figure 1). Five intermediates, designated S_0 to S_4, are formed by successive one-electron oxidations of the WOC. Each reaction center operates autonomously, with no or minimal sharing of redox equivalents. The S_0 and S_1 states are dark stable, while the S_2 and S_3 states are metastable; they spontaneously are reduced to the S_1 state in the dark by recombination with electrons from reduced electron acceptor or by diffusible reductants in the chloroplast. Thus, dark-adapted PSII samples consist of a mixture of the S_0 (25%) and S_1 (75%) states. The S_4 state is unstable and returns to the S_0 state with release of a molecule of dioxygen.

B. Proton Equilibria, S State Kinetics, and Activation Barriers

Early studies suggested that the four protons from the two substrate water molecules are released into solution in a 1−0−1−2 stoichiometry during S state transitions ($S_iY_z^+ \rightarrow S_{i+1}Y_z$).[33] Y_z^+ denotes the special tyrosine radical protein residue of PSII that is the precursor to oxidation of each S_i state).[19] Recent data, however, show a strong dependence of the proton stoichiometry and kinetics on the solution pH and the method of sample preparation.[34,35] Currently, the proton equilibria are thought to represent electrostatic effects on both ionizable protein residues (Bohr protons), in addition to substrate water proton ionization steps. Nevertheless, for all S state transitions except $S_2Y_z^+ \rightarrow S_3Y_z$, the rate of proton release accelerates in alkaline solutions between pH 6 and 7.5. This result suggests that an increase in the number or availability of proton acceptor sites at alkaline pH leads to faster oxidation of the WOC. If this interpretation is correct, then proton release is thermodynamically linked to oxidation of the WOC. This explanation suggests that substrate ionization of protons precedes dioxygen release on S_4. Alternatively, an electrostatic influence from ionizable residues or nonsubstrate water molecules on the electrochemical potential of the WOC may be another explanation.

The half-times for the S state advances $S_iY_z^+ \rightarrow S_{i+1}Y_z$ have been measured by direct observation of Y_z^+ reduction using EPR spectroscopy[36] and by following the electrochromic absorbance changes from chlorophyll in the UV−vis spectra.[37] For $i = 0, 1, 2$, the half-times vary between 30 and 350 μs, while the final rate-limiting step, $S_3Y_z^+ \rightarrow S_0Y_z + O_2$, has a half-time of approximately 1 ms. Activation energies for the S state transitions have been measured by Renger et al.[38] by measuring the temperature dependence of the kinetics of electrochromic absorption changes at 355 nm. Activation barriers of 5.0, 12.0, and 36.0 kJ/mol were measured and derived reorganization barriers (using Marcus' theory) of 0.05, 0.12, and 0.37 eV were found for the transitions $S_i \rightarrow S_{i+1}$ ($i = 0, 1, 2$). The reaction $S_3 \rightarrow (S_4) \rightarrow S_0$ had a temperature-dependent activation energy of 20 kJ/mol ($T > 279$ K) or 46 kJ/mol ($T < 279$ K) and a reorganization energy of 0.21 eV for the lower barrier step. The large barrier between the S_2 and S_3 states was interpreted as evidence for a major structural rearrangement. The weaker pH dependence of this transition (see last paragraph) suggests that the structural rearrangement may involve nuclear rearrangements other than proton release steps, or that such steps are not in equilibrium with solution protons. Recent EXAFS studies have indicated that a major structural change occurs which leads to an increase in inter-manganese separations.[39]

Messinger et al.[40] investigated the kinetics of substrate water exchange in the S_2 and S_3 states of PSII by using labeled ($^{18}OH_2$) water and time-resolved mass spectrometry. It was found that one water molecule slowly exchanges ($t_{1/2} \approx 0.5$ s at 10 °C) with solvent water in the S_2 and S_3 states, while another water molecule is either exchanging faster ($t_{1/2} < 60$ms) or enters only in the S_4 state (For comparison, permanganate (MnO_4^-) shows an extremely slow water-exchange rate of 0.5% of all oxo groups per hour at 25 °C in dilute, neutral solution.[41]) The slow-exchanging oxygen atom was proposed by the authors to be a terminal manganoyl (Mn═O) oxo, while the rapidly exchanging oxo is kinetically equivalent to a water molecule. However, there was no comparison to kinetic studies of aquo ligands exchange with Mn(III) or Mn(IV) model complexes to rule out this alternative assignment. This result shows that the two substrate water molecules bind differently in both the S_2 and S_3 states, either in two steps (S_2 and S_3) or at different sites. Furthermore, it was found that at least one substrate water molecule enters the active site before the S_4 state.

There is no direct evidence supporting oxidation of substrate water molecules prior to the $S_4 \rightarrow S_0$ transition in the native WOC; a concerted four-electron process is envisioned. However, certain treatments which block O_2 formation and S state advancement past S_3—including extraction of Cl^- or replacement of Cl^- by F^-—lead to significant release of hydrogen peroxide.[31,42−44] Thus, the two-electron oxidation path forming H_2O_2 and no direct O_2 production is favored, despite the additional increase in electrochemical potential from 0.82 to 1.35 V per electron. This result has been interpreted via a model that proposes a role for Cl^- in promoting intracluster electron transfer via redox poising of Mn, mediated by coordination to the special "gateway" Mn site, possibly at a bridging site between Mn ions.[31]

C. Tyrosyl Radical Participation in Water Oxidation?

Several experiments have demonstrated that an unstable radical can be photogenerated in close proximity to the Mn cluster in PSII membranes following a variety of treatments which block normal O_2 evolution at the S_3 state, including extraction of the Ca^{2+} or Cl^- cofactors, Cl^- replacement by F^-, or acetate treatment.[45−48] Recently, it has been demonstrated rather conclusively by isotopic labeling studies using deuterated tyrosines that the radical is Y_z and that it may be located as close as 4.5 Å from the tetramanganese cluster.[24,49] These results support a new metalloradical mechanistic model for oxygen production based on the possible involvement of Y_Z in proton[24,49] or H atom[23,50] abstraction from substrate water molecules bound to the tetramanganese cluster. In this model Y_Z serves to abstract an electron and proton from the substrate−tetramanganese complex on each of the S state transitions. Depending on the degree of coupling between the substrate molecule and the tetramanganese core, the oxidation step could involve either formal H atom transfer from water or uncoupled proton/electron transfer from the substrate−tetramanganese complex. At present, this model is based solely on the physical proximity between Y_Z and the tetramanganese complex. Here, a thermodynamic analysis is given based on recent studies indicating that quantitative predictions can be made about the rate of H atom transfer reactions to metal−oxo coordination complexes.

Oxidation of C−H bonds in organic substrates by oxo-containing coordination complexes of chromium

Scheme 1. Proposed Mechanisms[a]

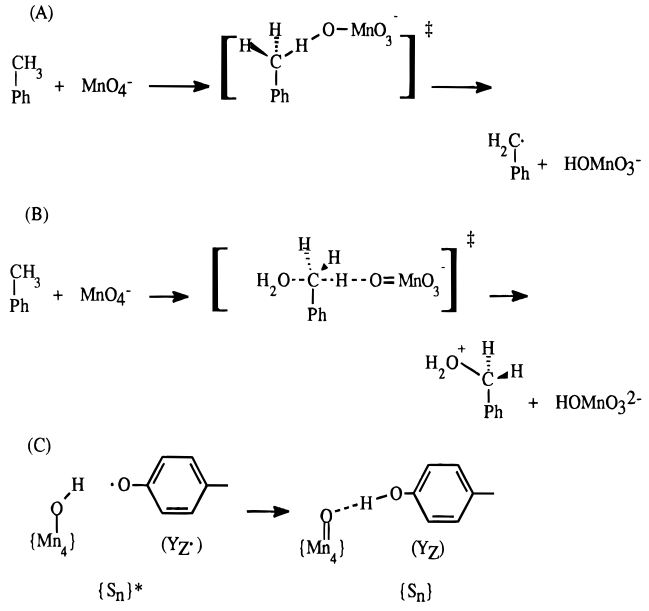

[a] (A) Proposed mechanism of hydrogen atom transfer and (B) hydride transfer in the reduction of permanganate by toluene.[21] (C) Conjectured mechanism of hydrogen atom transfer to tyrosyl radical (Y_Z•) from the substrate−tetramanganese complex of photosystem II (adapted from refs 23 and 24).

(CrO_2Cl_2) and permanganate (MnO_4^-) has been found to occur either by hydrogen atom transfer (in nonpolar solvents) or by hydride transfer (in aqueous solvent).[21] An H atom transfer mechanism was found to operate in neat toluene (Scheme 1A). A linear correlation was observed between the kinetics of H atom transfer to permanganate and the reaction enthalpy change for C−H bond dissociation minus H−O bond formation ($\Delta\Delta H°_{rxn}$). This correlation included a number of oxygen radicals (OH•, ^{t}BuO•, and ^{t}BuOO•) and a nonradical oxidant (MnO_4^-) and extended over an impressive 16 orders of magnitude in rate. The bond strength of the O−H bond formed upon H atom transfer to permanganate was estimated to be 83 kcal/mol[21] and more recently 79 kcal/mol,[51] using a thermochemical cycle based on the measured values for the reduction potential, the pK_a of the reduced oxidant, and the standard bond enthalpy of molecular H_2 (56 kcal/mol).[52] Thus, permanganate, a nonradical oxidant, reacts just as one would predict for an oxygen radical that makes a 79 kcal/mol bond with an H atom. A general conclusion reached from this study is that H atom abstraction reactions can occur with metal−oxo oxidants, regardless of their radical character, provided there is a high thermodynamic affinity for the H• atom. Importantly, when the nonpolar solvent was changed by adding water, the H atom transfer reaction was not observed, owing to a 1000-fold faster, lower energy, hydride transfer reaction to permanganate that is coupled to hydration of the incipient toluyl carbocation (Scheme 1B). This two-electron/one-proton pathway dominates in more polar solvents, owing to both a smaller enthalpy increase and a larger entropy decrease compared to H atom transfer. This indicates that there are at least two relatively low-energy mechanisms for oxidation of C−H bonds by oxo−metal complexes which may operate under different conditions depending on solvent polarity and availability of water.

We can extend these ideas to predict the theoretical rate of H atom abstraction by a tyrosine radical from the O−H bond of various hydroxo−manganese complexes which may share structural features in common with the WOC (Scheme 1C). To do this, we will use the same correlation between $\Delta\Delta H°_{rxn}$ and rate constant as was established for C−H bond oxidation in nonaqueous solvent. $\Delta\Delta H°_{rxn}$ is calculated as the difference in bond dissociation enthalpies for the O−H bond in the reduced manganese complex vs the tyrosine O−H bond.

The reduction potential for the neutral tyrosyl radical in dilute aqueous solution has been accurately determined by pulse radiolytic methods to be 0.94 ±0.01 V vs NHE at pH 7 and 25 °C.[53] The pK_a of tyrosine in solution is 9.11 (vs 9.89 for phenol) at 20 °C.[54] Using these values and the aforementioned thermodynamic cycle, we obtain a bond dissociation energy of 90±1 kcal/mol for the phenoxyl O−H bond in tyrosine in dilute aqueous solution, in excellent agreement with an earlier estimate.[55] Using the same method a mean value of 90 ±1 kcal/mol was calculated for the average O−H bond energy in phenol and its 3-Me, 3,5-diMe, 4-Cl and 4-Br derivatives in nonaqueous solvents.[52]

The computed μ-(O−H) bond enthalpies for three different μ-hydroxo-μ-oxo bridged complexes, Mn_2(III,IV)(μ_2-OH,O)L_4, are given in Table 1. These were computed using a thermochemical cycle, from the published reduction potentials and pK_a values for both the (III,III)/(III,IV) and (III,IV)/(IV,IV) redox couples.

The enthalpy change for H atom transfer ($\Delta\Delta H°_{rxn}$) from each of the $Mn_2(\mu_2$-OH,O)L_4 complexes to the tyrosyl radical (analogous to Scheme 1C) can then be calculated using the data in Table 1 and the tyrosine O−H bond dissociation enthalpy. The results are listed in Table 2, along with the predicted bimolecular rate constants for H atom transfer, assuming the same linear correlation between these two quantities established for C−H bond oxidation.[21] (See Note Added in Proof at the end of this review.) These predicted rate constants would apply to the indicated dinuclear complexes if they were to behave just like permanganate and the oxy radical oxidants.

The predicted bimolecular rate constant is considerably faster for H atom abstraction from the Mn_2(III,IV) (lower) oxidation state than from the Mn_2(IV,IV) state, regardless of the ancillary ligands. This is because of the stronger μ-(O−H) bond in the more oxidized complexes. Comparison of complexes in the same oxidation state shows that the more basic the μ-oxo atom is (the higher pK_a), the slower is the predicted transfer rate (Table 2). A 5-fold slower rate is predicted for each pK unit increase according to the correlation. This decrease in rate with increasing μ-oxo basicity also originates from an increase in the μ-(O−H) bond strength (Table 1). The data show that the ancillary ligands play a major role in determining both the reduction potential and the basicity of the μ-oxo atom, as is well-known for structurally analogous complexes.[20] For comparison, the rate of H atom transfer from hydrogen manganate ($HMnO_4^-$)

Table 1. Reduction Potentials[a], pK_a Values[a,b] and Deduced[c] O−H Bond Dissociation Energies for Dinuclear Complexes

complexes[e]	oxidation state	$E_{1/2}$ III:IV/III:III	pK_a III,III[b]	$\Delta H°$ III,III[b]	$E_{1/2}$ IV:IV/III:IV	pK_a III,IV[b]	$\Delta H°$ III,IV[b]
$Mn_2(O)_2(bpy)_4^{3+}$	III,IV	0.53	11.0	−83	1.49	2.3	−93
$Mn_2(O)_2(phen)_4^{3+}$	III,IV	0.57	9.15	−82	1.53	(0.4)[d]	−92
$Mn_2(O)_2(bispicen)_2^{3+}$	III,IV	0.38	8.35	−76	0.99	(−0.4)[d]	−78
MnO_4^-	VII	0.564[f]	10.5[f]				

[a] In volts vs NHE.[18,19] [b] For the corresponding conjugate acid (μ_2-O, OH) in aqueous solution. [c] Determined from $E_{1/2}$ and pK_a values using the thermodynamic cycle in Scheme 2. [d] Estimated from the measured pKa for the (III,III) species and applying a ΔpK_a(III,III−III,IV) = 8.7 shift, as observed experimentally for $Mn_2(O)_2(bpy)_4^{3+}$. This trend is supported in related oxo−manganese complexes.[20] [e] bpy = 2,2′-bipyridine; phen = 1,10-phenanthroline; bispicen = *N*,*N*′-bis[2-methyl-1-pyridylethane-1,2-diamine]. [f] Refers to the one-electron reduction to manganate and its associated proton ionization of $HMnO_4^-$.

Table 2. Calculated Enthalpy ($\Delta\Delta H°_{rxn}$)[a] and Predicted Rate Constant (k)[b,c] for a H Atom Transfer Reaction[d,e] between Neutral Tyrosyl Radical and the O−H Bond in Dinuclear Complexes and Permanganate

complex	$\Delta\Delta H°_{rxn}$:k (III,III)[d]	(III,IV)[e]
$Mn_2(O)(OH)(bpy)_4^{3+/4+}$	−7:2	$3:2 \times 10^{-5}$
$Mn_2(O)(OH)(phen)_4^{3+/4+}$	−8:10	$2:1 \times 10^{-4}$
$Mn_2(O)(OH)(bispicen)_2^{3+/4+}$	−14:5000	−12:600
$HOMnO_3^{2-}$ (permanganate)[f]	−11:200	

[a] kcal/mol. [b] M^{-1} s^{-1}. [c] Polanyi plot: $\log k = -0.49(\Delta\Delta H°_{rxn}) - 3.0$ (ref 21). [d] (III,III)(OH) + $Y_Z^•$ → (III,IV)O + Y_ZH. [e] (III,IV)(OH) + $Y_Z^•$ → (IV,IV)O + Y_Z. [f] $HOMnO_3^-$ + $Y_Z^•$ → MnO_4^- + Y_Z.

to the tyrosyl radical is predicted to occur with a rate constant of 200 M^{-1} s^{-1}, based on its O−H bond dissociation energy of 79 kcal/mol.

The pseudo-first-order rate constant for H atom transfer in a concentrated nondiffusing system can be arrived at by multiplying the bimolecular rate constant by the effective concentration of reacting partners. This concentration is approximately 10 M for the case of Y_Z and the tetramanganese cluster. (10 M is arrived at using an isotropic model with approximate molecular volumes for Y_Z and the {Mn_4} cluster and a distance of separation of 4.5 Å.) We shall compare the pseudo-first-order rate constants with the known rate constants for $Y_Z^•$ radical reduction observed in the WOC to see if H atom transfer should be considered as a possible mechanism ($S_nY_Z^•$ → $S_{n+1}Y_Z$; $k = 2 \times 10^4$ to 7×10^2 s^{-1}). We also restrict the choice of hydroxo−manganese complexes to those which have a pK_a above the observed pK_a for the S state transition, $S_nY_Z^•$ → $S_{n+1}Y_Z$; otherwise, the μ-oxo group would not be protonated and there would be no H atom transfer pathway to consider. On the basis of the observed pK_a values given in Table 2, we see that all three $Mn_2^{III,IV}$(O)(OH) complexes would be unprotonated at pH ≥ 3, existing as the di-μ-oxo form, and thus unavailable for H atom transfer. Therefore, we eliminate this oxidation state from further consideration.

Next we consider the three (III,III) examples given in Table 2. Only the bispicen complex has a sufficiently rapid H atom transfer rate (5×10^4 s^{-1}), while the other two complexes are a factor of 10−100 times too slow (k = 20−100 s^{-1}). All of these complexes have pK_a values that would ensure that they have protonated μ-(OH) in the physiological range observed for the S state transitions. Thus, we see that H atom transfer to tyrosine from Mn_2(O)(OH)$^{3+}$ for the (III,III) to (III,IV) oxidation step might be fast enough to consider as a viable mechanism for S state transitions, but only for Mn complexes which are particularly weak oxidants (viz. $E_{1/2}$ = 0.38 V vs NHE for the bispicen complex). However, it is very unlikely that such weak oxidizing potentials exist for any of the S state transitions which most likely fall at or above the potential of the auxilliary tyrosine radical $Y_D^•$ that is in equilibrium with the WOC.[28]

We reach the conclusion that the predicted rate of H atom abstraction from the substrate−WOC complex by $Y_Z^•$ appears not be fast enough to be functionally important *in vivo*. Model complexes with sufficiently high pK_a values to have bridging hydroxyl groups and reduction potentials in the range of the WOC are predicted to have H atom transfer rates that are too slow to account for the observed S state kinetics in PSII. Despite the appeal that H atom transfer may have based on the physical proximity of the cofactors, there does not appear to be a strong thermochemical basis to support its occurrence in photosynthetic water oxidation. It is important to note that these are predictions based on the observed kinetics of H atom transfer from C−H bonds. It would be useful to measure directly the rates of O−H bond cleavage in model Mn complexes before a definitive answer is given.

Comparison with more ionic mechanisms customarily associated with oxidation of polar O−H bonds, like water bound to strong Lewis acid metal centers, should be considered. Recall that an ionic mechanism involving hydride transfer is favored in water over H atom transfer for C−H bond oxidation. An alternative proposal for the rate-limiting step is to reconsider "uncoupled" or "weakly coupled" electron/proton transfer in which Y_Z acts as a traditional one-electron transfer agent and substrate protons are transferred to other sites in the WOC that are either uncoupled or only weakly coupled to reprotonation steps of the reduced Y_Z^- (tyrosinate) anion. This more polar mechanism would be favored in aqueous solvents compared to a H atom transfer mechanism, by analogy to oxidation of the C−H bond in aqueous toluene by permanganate (Scheme 1B).

Lastly, it is difficult to imagine how the close physical juxtaposition necessary for H atom transfer from Y_Z to two water molecules bound at different sites in the WOC could exist on each of the four sequential S state transitions. Although, there is inadequate stereochemical data to address this question at present.

D. Electronic and Coordinate Structure of the WOC

Electronic and nuclear structural information about the WOC has come primarily from EPR and XAS spectroscopies. The S_2 oxidation state exhibits a multiline EPR signal attributed to a spin-coupled tetramanganese cluster having a ground state with doublet spin character $S = {}^1/_2$. The oxidation states of the manganese ions in the S_2 state were predicted to be (3III,IV), based on EPR measurements of ^{55}Mn hyperfine couplings[56−58] and Mn X-ray absorption edge analysis,[59] or alternatively (III, 3IV), based on XAS analysis.[60,61] These lead to predicted oxidation states for the O_2-evolving S_4 state of (2III,2IV) + Y_z^+ and (4IV) + Y_z^+. Reduction of Y_z^+ in S_4 is kinetically indistinguishable from O_2 release, so there is no evidence yet for direct oxidation of Mn on the $S_3 \rightarrow S_4$ transition. Oxidation of Mn on all transitions other than $S_2 \rightarrow S_3$ has been proposed on the basis of Mn X-ray absorption edge studies.[62] However, since it is now known that a structural change accompanies the $S_2 \rightarrow S_3$ transition, the edge energy is not a clear reporter of the oxidation state change for this transition. UV optical changes have also been used to suggest oxidation state changes of Mn. But these too have been shown to be complex, reflecting the net accumulation of charge and electrochromic effects. Most data, including EPR, have supported sequential oxidation of individual Mn ions on the $S_0 \rightarrow S_1$ and $S_1 \rightarrow S_2$ transitions. For higher S state transitions, it is less clear whether Mn or an amino acid residue is the site of oxidation.

Mn EXAFS studies have revealed two distances of 2.73 and 2.85 Å in the S_1 state attributed to two Mn_2-(μ-O)$_2$ cores.[63] A second shell at 3.3 Å has been interpreted in various ways: either another shell of 0.5 Mn or Mn + Ca scattering atoms per Mn absorber, including possible contributions also from multiple scattering effects from C (light) atoms (summarized in refs 28 and 64). The lack of agreement concerning the origin of the 3.3 Å scattering shell, combined with the inability of EXAFS to detect the three Mn−Mn scattering vectors in the cubanes (Mn_3O_3X, X = Cl, Br),[1] indicates that only the 2.7−2.8 Å structural feature can be assigned with confidence. The error in the predicted coordination number of atoms responsible for each scattering vector increases with distance; the average first-shell coordination number for Mn has been estimated to be 6 ± 1 atoms. The first shell is proposed to be due to the presence of two short di-μ-oxo bonds and four other O or N atoms on the basis of comparisons with model complexes, many of which were synthesized in the 1980s and used as structural models for the WOC.[1] Some core structures of these model complexes are shown in Figure 2.

On this basis, the di-μ-oxo core present in $[Mn_2O_2]^{3+/4+}$ complexes and the mono-μ-oxo-mono-(or bis)-μ-carboxylato core present in $[Mn_2(O)(O_2CR)_{1-2}]^{2+/3+/4+}$ complexes were proposed to be structural candidates for the 2.7−2.81 and 3.3 Å Mn−Mn vectors in the WOC, respectively. EXAFS studies by Penner-Hahn et al. have revealed a distribution of first shell distances without clear evidence for the (μ-O)$_2$ unit.[65] Despite the inconsistencies pointed out above, the four structural models depicted in Figure 3 have been proposed.

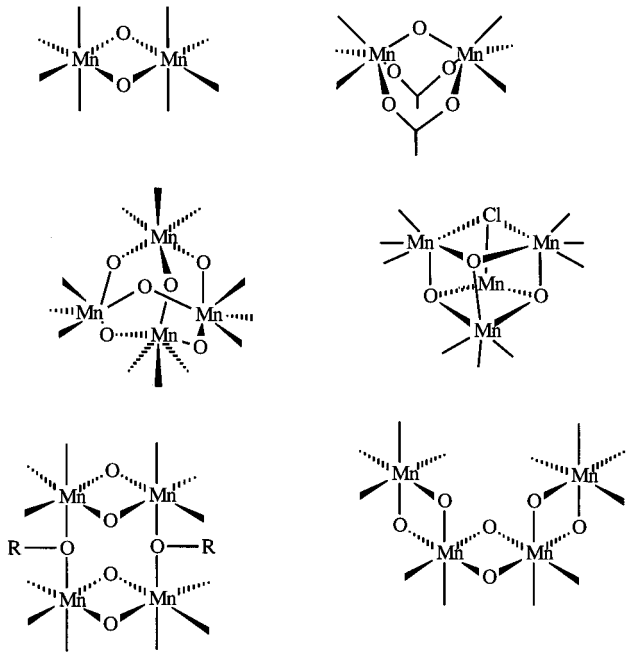

Figure 2. Synthetic Mn−oxo core structures that have been proposed as speculative models for the WOC.

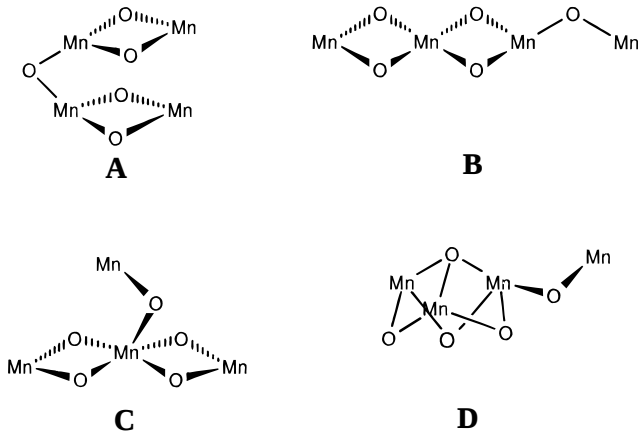

Figure 3. The "Berkeley" models of the WOC, based primarily on EXAFS data.[1]

A lower coordination number of five for the Mn(III) ions in the S_2 state has been indicated by EPR spectroscopy, most likely a distorted trigonal bipyramidal ligand geometry or less likely six ligands in a tetragonally compressed ligand geometry (reverse Jahn-Teller distortion).[31,56,57] The lower coordination number may offer a possible explanation for the discrepancy in Mn oxidation state assignments noted above. The oxidation states assigned by XAS (III, 3IV) were made by comparison primarily to six-coordinate rather than five-coordinate model complexes and thus should lead to higher predicted oxidation states.

Based on the observed strong antiferromagnetic coupling within the di-μ-oxo cores [both $Mn^{IV}(\mu\text{-O})_2Mn^{IV}$ and $Mn^{III}(\mu\text{-O})_2Mn^{IV}$] and the much weaker exchange coupling within mono-μ-oxo cores [$Mn^{III}(\mu$-O)Mn^{III} and $Mn^{III}(\mu$-O)Mn^{IV}, both antiferromagnetic

types observed], Zheng et al. attempted to use the dimer-of-dimers structural model to construct an effective magnetic model that could explain the multiple forms of the S_2 state multiline EPR signal.[56,57] Although a dimer-of-dimers magnetic model was successful in interpreting the spectra, it required the presence of two ferromagnetic dimers, which when related to the Berkeley structural model required assignment of the two putative di-μ-oxo dimers to ferromagnetic pairs. The magnetic model implies the existence of two relatively strong ferromagnetic interactions, a feature requiring a tetranuclear structure that is inconsistent with the dimer-of-dimers and linear structural models given in Figure 3A,B. Thus, the structural model, predicting two weakly associated $Mn_2(\mu\text{-}O)_2$ cores, and the magnetic model, predicting a more strongly interacting magnetic tetramer, cannot yet be reconciled with any of the available tetranuclear model complexes.

III. Proposed Models for Water Oxidation by PSII

Many speculative proposals have been made for the mechanism of photosynthetic water oxidation, dating back as far as 1970 (summarized in ref 66). The 1980s saw big advances in manganese coordination chemistry which spawned new proposals. In 1986, Brudvig and Crabtree published a mechanistic proposal,[2] based on structurally characterized Mn complexes, followed shortly thereafter by a proposal by Vincent and Christou in 1987.[3] The mechanisms are based partially on experimental structures, like the known (Mn_4O_6) adamantane-type, (Mn_4O_3X) cubane-type, and (Mn_4O_2) butterfly-type Mn_4 cores. They share the idea of incorporation of substrate water molecules into the cluster as bridging oxo groups as the proposed mode for activation of substrate. In each mechanism, two structurally equivalent oxo atoms couple to form dioxygen upon cluster rearrangement to re-form the starting cluster. These mechanisms have been reviewed[67,68] and only recent insights will be discussed.

Brudvig and Crabtree's mechanism is depicted in Figure 4a. Rearrangement of an unprecedented Mn_4O_4 cubane was proposed as the basis for the mechanism. Since then, Christou's $[Mn^{III}{}_3{}^{IV}{}_4O_3Cl]^{5+}$ distorted-cubane complex,[69] has been reported and thus provides a structural precedent, although no Mn_4O_4 cubanes are known yet. Interestingly, the unknown Mn_4O_4 cubane structure was used by both groups as a key intermediate in their proposals. The oxidation state of the Mn_4O_3Cl complex is appropriate for the S_2 oxidation state of the WOC, but the magnetic properties show that it has an $S = {}^9/_2$ ground state, as compared to the $S = {}^1/_2$ ground state for the native S_2 state and $S = {}^3/_2$ or ${}^5/_2$ for the modified $g = 4.1$ form of the S_2 state. A structural change in the "cubane" structure could alter the ground state to give $S = {}^7/_2$, ${}^5/_2$, ${}^3/_2$, or ${}^1/_2$ ground states, as pointed out by Wang et al.[70] In Brudvig and Crabtree's proposal, the cubane structure is oxidized from S_0 to S_2 without rearrangement. This agrees with the most recent Mn EXAFS data on the WOC indicating little structural change prior to the S_3 state. Subsequent oxidation of the S_2 state to S_3 triggers the binding and deprotonation of two substrate water molecules to form the adamantane core. The resulting adamantane structure resembles model complexes by Wieghardt et al.[68] Further oxidation is proposed to result in dioxygen release and relaxation to the S_0 cubane structure. The O−O bond formation is proposed to occur between bridging oxo groups with possible formation of a peroxo intermediate. Since the proposal was made it has been pointed out that the symmetric adamantane core structure is incompatible with Mn EXAFS data.[1] Moreover, the proposed mechanism suggests that the adamantane core is reactive toward elimination of O_2 and formation of the more stable Mn_4O_4 cubane. This is contrary to the available data on model complexes, which indicates that the adamantane core is a thermodynamic sink into which the Mn_2O_2 and Mn_4O_2 cores often revert to upon oxidation.[68] Furthermore, the recent studies of substrate water exchange in the S_2 and S_3 states (vide supra) contradict the notion of dioxygen elimination from equivalent μ-oxo groups.

Vincent and Christou's proposed "double-pivot mechanism"[3] is given in Figure 4b. The basic features are similar here. A structural rearrangement takes place between the S_2 and S_3 states, increasing the number of bridging oxo groups by two. The structurally characterized "butterfly" and distorted-cubane (Mn_4O_3Cl) structures provide the basis for this mechanism. Two water molecules are proposed to bind in the S_2 state.[71,72] The observed oxidation-induced incorporation of oxide anion (from water) into the Mn_4O_2 butterfly to give the $Mn_4O_3(O_2CR)$ cubane-like core[70] has led to a new mechanistic proposal. The cubane-like core is derived from the trigonal Mn_4O_3Cl core by replacement of the triply bridging μ-Cl^- by a carboxylate bridge between the three Mn(III) ions, as shown in Figure 4c (top right insert). In the new proposal (Figure 4c), all S states are represented by a cubane-like Mn_4O_3 core. Especially the proposed S_2 state is similar to the model complex described above, with the exception that the carboxylate bridge is replaced by a hydrogen-bonded water molecule−μ-oxide (μ-O···H−O−H) group. The O−O-bond formation takes place between a terminal and a bridging oxo group. This chemical difference between the oxo groups could also explain the different exchange rates for the two substrate water molecules in PSII, although there is very limited exchange data on model oxo's to support this hypothesis.

In 1993, Proserpio et al. proposed a model for photosynthetic oxygen evolution, based on a "hybrid" of the Berkeley "dimer-of-dimers" model and an experimental structure of a Mn(II,3III) tetramer (Figure 5).[73] The tetranuclear unit of the experimental structure shows a unique hydrogen-bonded μ_4-O−H−O unit with the two oxygens at a distance of 2.42 Å. The complex exhibits catalase activity much like the S_0 state of PSII in the dark and has the same oxidation states (II, 3III) as proposed for the S_0 state of PSII. Initial speculation that an O−O bond could form by coupling the μ_4-O−H−O group after deprotonation was dismissed in this work,[74] because the resulting peroxo complex would have a nonequilibrium structure on the basis of force field calculations.[4] In the proposed model, dioxygen formation takes

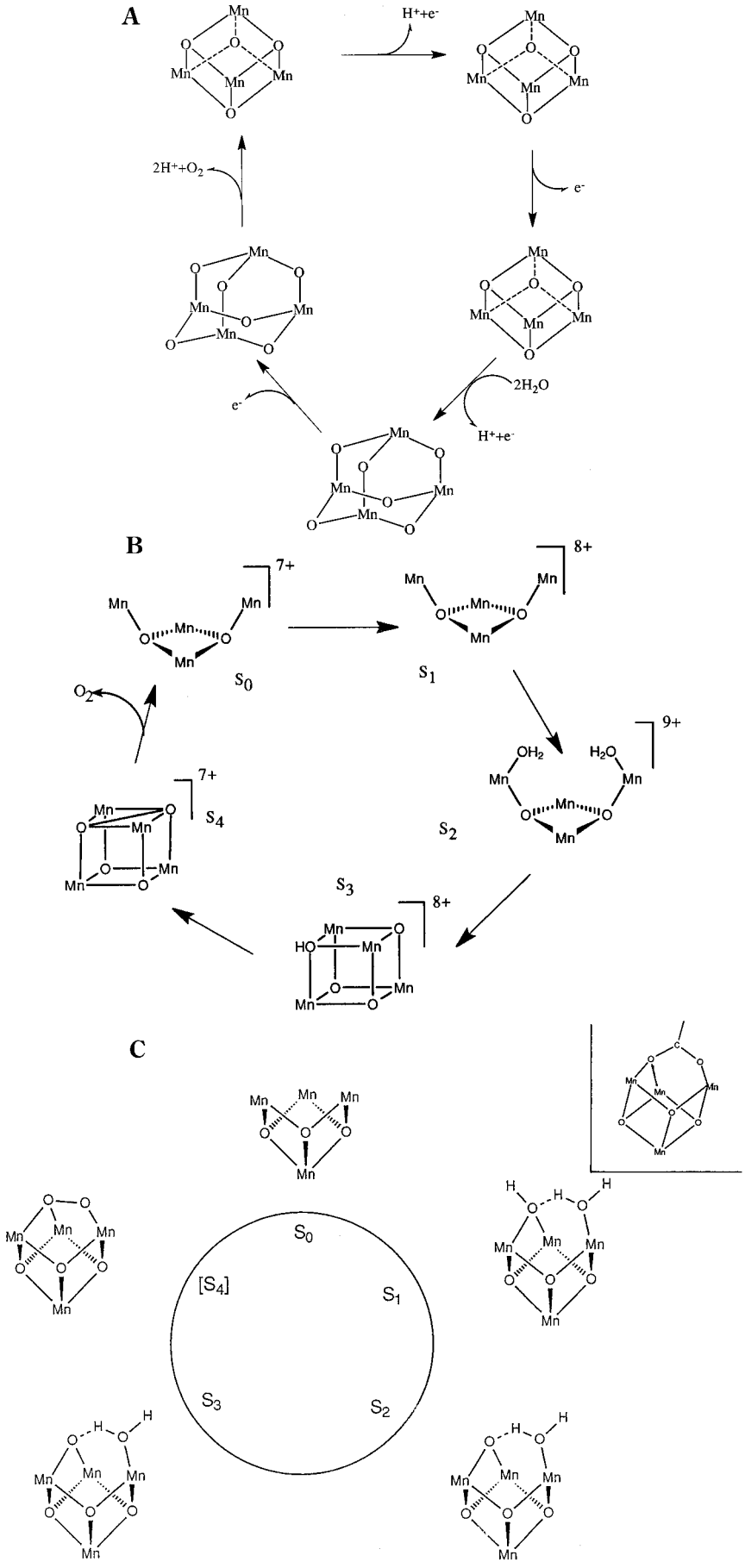

Figure 4. (a) model cycle for water oxidation proposed by Brudvig and Crabtree.[2] (b) Model cycle for water oxidation proposed by Vincent and Christou.[3] (c) Modified model by Christou et al. The structure of an experimentally characterized cubane-like core is shown in the top right insert. (Figure kindly provided by Prof. Christou.)

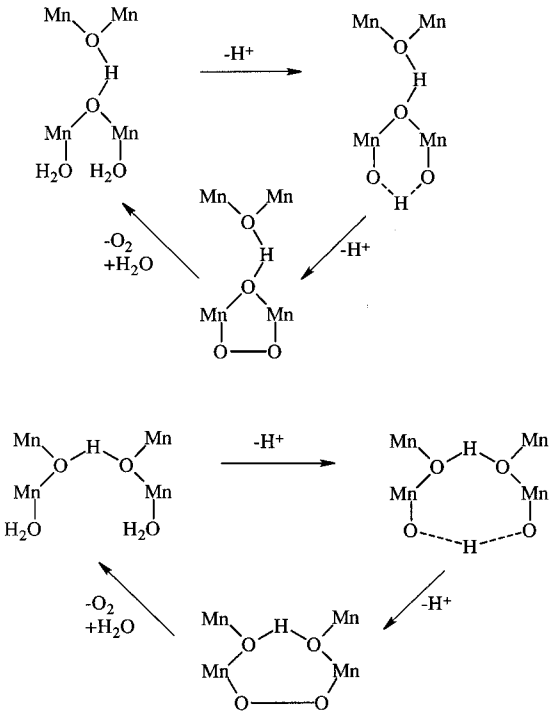

Figure 5. Model for the oxidation of water by the WOC based on Hückel calculations.[4]

place in two two-electron steps with bound peroxide as an intermediate, as depicted in Figure 5. The μ_4-O−H−O group plays no direct role in O−O bond formation, other than to provide an interaction pathway between the two Mn_2O dimers needed for charge delocalization. Deprotonation of terminal aquo ligands leads to O−O coupling and eventually release of dioxygen from one dimer of the tetramer. Here again, symmetrical terminal oxos are involved in O−O bond formation, a feature inconsistent with the very different water exchange rates for the two oxo atom precursors of the WOC.

IV. Thermodynamics of Water Oxidation

A. Concentration-Independent Configuration Potentials

The oxidation of water to molecular oxygen (eq 1) involves the transfer of four electrons from water to an oxidant, coupled with the release of four protons.

$$2H_2O \rightarrow O_2 + 4H^+ + 4e^- \qquad (1)$$

Conceptually, this process can occur as a concerted four-electron reaction, or in multiple steps of one to three electrons with the formation of stabilized intermediates that are bound to the catalyst. These are the hydroxyl radical, peroxide, and superoxide radical. The intermediates would in turn be further oxidized to molecular oxygen. Figure 6 plots the relevant redox potentials as a function of pH in aqueous solution together with the potentials of two common oxidants, $Fe(bpy)_3^{3+}$ and $Ru(bpy)_3^{3+}$. A few general points can be made from this picture. The OH radical is the highest energy species, and all other species in the diagram can be created from it by spontaneous disproportionation and reduction reactions. The four-electron reduction of dioxygen to water has the smallest thermodynamic driving force. Therefore, the reverse reaction, the four-electron

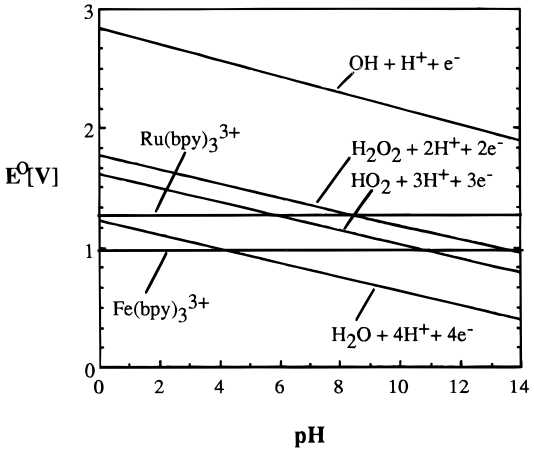

Figure 6. The pH dependence of the standard reduction potentials for oxygen and its reduced forms. As a reference, the potentials of two standard oxidants ($Ru(bpy)_3^{3+}$ and $Fe(bpy)_3^{3+}$) are included.

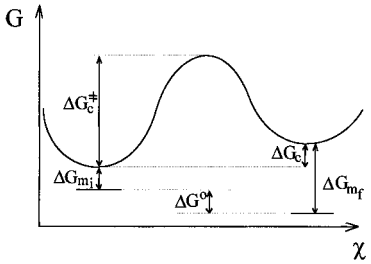

Figure 7. The free energy change during the course of a chemical reaction (solid line) as the basis for the definition of the configurational potentials. The free energy of the reactants (i) and products (f) differ from the value in solution by the free energy of solvation.[5]

oxidation of water, should have the lowest thermodynamic barrier. However, this picture of standard reduction potentials is misleading in several aspects.

As Krishtalik pointed out,[75] the low oxidation potential of water at pH 7 is mainly due to the favorable free energy of mixing of final products (mainly H^+) in the solution (where $[H^+] = 10^{-7}$ M). However, there is no bulk water present in the active site of PSII and the pH as well as p*K* values therein are not known. Therefore, it is better to consider the configurational potentials, which are independent of concentration (and therefore of pH) and only include the change in free energy in the elementary step.[5] This is illustrated in Figure 7, showing the change in free energy for a single elementary reaction (solid line) and the accompanying free energy changes for mixing of the reactants and products in the bulk solution. The minima in the free energy curves do not correspond to the energy levels of reactants (i) and products (f) in solution. The energy differences ΔG_{mi} and ΔG_{mf} arise from the dilution of the reactants (i) and products (f) in the solution, respectively. The configurational free energy change for the elementary reaction, ΔG_c, is obtained as follows:

$$\Delta G_c = \Delta G^\circ + \sum RT \ln x_i^\circ + \sum RT \ln x_f^\circ \qquad (2)$$

[x being the molar fractions of reactants (i) and products (f).] The corresponding elementary redox potentials, $E_c = \Delta G_c/nF$), are listed in Table 3 for various oxidation reactions.

Table 3. Measured Standard Reduction Potentials in Aqueous Solution (pH = 0) and Calculated Configurational Potentials for the Elementary Reactions Assuming Ideal Entropies of Mixing[5,22]

reaction	standard E_0	config E_c
Four-Electron Reactions		
$2H_2O \rightarrow O_2 + 4H^+ + 4e^-$	1.229	1.401
$OH^- + H_2O \rightarrow O_2 + 3H^+ + 4e^-$	1.022	1.142
$2OH^- \rightarrow O_2 + 2H^+ + 4e^-$	0.815	0.884
$4OH^- \rightarrow O_2 + 2H_2O + 4e^-$	0.401	0.367
Two-Electron Reactions		
$2H_2O \rightarrow H_2O_2 + 2H^+ + 2e^-$	1.776	1.931
$2OH^- \rightarrow H_2O_2 + 2e^-$	0.948	0.896
$H_2O_2 \rightarrow O_2 + 2H^+ + 2e^-$	0.682	0.870
$H_2O_2 + 2OH^- \rightarrow O_2 + 2H_2O + 2e^-$	−0.146	−0.163
One-Electron Reactions		
$H_2O \rightarrow OH + H^+ + e^-$	2.848	3.225
$OH^- \rightarrow OH + e^-$	2.020	2.191
$H_2O_2 \rightarrow HO_2 + H^+ + e^-$	1.495	1.598
$H_2O_2 + OH^- \rightarrow HO_2 + H_2O + e^-$	0.667	0.564
$HO_2 \rightarrow O_2 + H^+ + e^-$	−0.130	0.144
$HO_2 + OH^- \rightarrow O_2 + H_2O + e^-$	−0.958	−0.890

Here, the four-electron oxidation of water has a potential of 1.4 V, which is considerably higher than the primary oxidant for the Mn cluster in photosynthesis, tyrosine Y_z, with a potential estimated to be 1.1 V. How then can photosystem II oxidize water? One could argue that the elementary step could well be uphill and that the favorable energy for release of O_2, electrons, and protons into solution (or elsewhere) is used to drive this step. Calculation of the fastest reaction time for the elementary step alone using the Eyring equation,

$$k = \frac{k_B T}{h} \kappa \exp \frac{-\Delta G_c^{\ddagger}}{RT}$$

with $\kappa = 1$ and assuming the energy barrier to be (1.4 V − 1.1 V) × 4 V = 1.2 V (this energy is the difference between the configurational potential for the four-electron oxidation of water and the potential of Y_z^+), yields 10^7 s for the reaction time (which gives $1/k$, and therefore $k = 10^{-7}$ s^{-1}).[5] This is quite unrealistic, since the rate-limiting step in photosynthesis ($S_3 \rightarrow S_0 + O_2$) was determined to have a reaction time of 10^{-3} s ($k = 10^3$ s^{-1}).[76]

One factor which can reduce the potential required for water oxidation considerably is binding of the released protons by bases with p$K > 7$ (ref 5). There are, in principle, two ways to incorporate this concept: either one raises the energy of the reactants by oxidizing OH^- instead of H_2O (substrate deprotonation prior to oxidation) or the released protons must bind to a good base, which lowers the energy of the reaction products. Table 3 shows that using OH^- instead of H_2O as the reactant lowers the configurational potential to 1.14 and 0.88 V, substituting one or two OH^- for water molecules, respectively. On the other hand, to ensure a high local concentration of OH^- in the active site, these should be bound to Mn or Ca ions or other cationic protein residues. Another method of lowering the potential is to incorporate external bases (B, located in the active site) other than water in the reaction, according to the equation

$$2H_2O + 4B \rightarrow O_2 + 4BH^+ + 4e^- \qquad (3)$$

Scheme 2. Scheme for the Thermodynamic Analysis of Water Oxidation and the Involved Proton-Transfer Steps[25]

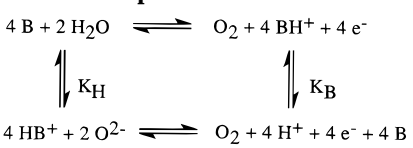

The change in the free energy arising from protonation of B instead of water can be obtained from eq 4.[25]

$$\Delta G_{obs} = \Delta G°_{H^+} - RT \ln[1 + 10^{(pH - pK_B)}] \qquad (4)$$

This equation is obtained from the thermodynamic cycle for the ionization and proton transfer reactions shown in Scheme 2.

$\Delta G°_{H^+}$ (113.3 kcal/mol, pH = 0) is the limiting free energy change for the reaction at low pH where B is completely protonated and water is the only available proton acceptor. For one pH unit above the p$K_A(BH^+)$ (acid dissociation constant) of base B eq 4 predicts ΔG_{obs} will change by −1.0 kcal/mol at $T = 300$ K. An equal increase of opposite sign in ΔG occurs upon shifting the pH one unit below the pK_A. The corresponding configurational free energy change $\Delta G_{obs(c)}$ is obtained by using eq 2.

Bases of high p$K_A(BH^+)$ that are in rapid exchange with the solution at neutral pH will be mostly protonated and not available for proton binding. One attractive way to circumvent this potential problem is to use the increase in ligand basicity upon reduction of the metal cluster during water oxidation. Metal ligands could then serve as bases to bind protons that are released during water oxidation. In particular, water in the coordination sphere of aquo Mn(III) has a pK of about 0, so one water molecule would be deprotonated under physiological pH. Upon reduction to Mn(II), the pK would rise to about 10.5 and the deprotonated water ligand could serve as an effective base, driving the overall reaction via these proton-coupled electron transfer steps. Using eq 4 and this ΔpK_A of 10.5, the contribution to the free energy change arising from this proton transfer reaction is $\Delta(\Delta G) = 4.81$ kcal/mol (similar arguments would hold for Mn-bound His residues). Thus, by coupling proton release and binding of these protons by a good base to the oxidation reaction of water it is possible to drive the intrinsically unfavorable oxidation process.

The sequential 2 × 2e$^-$ pathway via peroxide has a higher oxidation potential for the initial step by 534 mV, compared to the concerted 4e$^-$ pathway (Figure 6). This difference could be compensated (in part) by stronger binding of the intermediate peroxide relative to two water molecules.[5] However, this binding energy must be lost in the next two-electron step, otherwise tight binding of the O_2 product would have to be assumed. Tight binding would lead to slow O_2 release and slow down the catalytic cycle. The rate-limiting step of photosynthetic dioxygen evolution is the $S_3 \rightarrow S_0 + O_2$ step, with a rate constant of about 10^3 s^{-1}. This relatively slow rate would allow for such an uphill step. On the other hand, the measured activation barrier from the

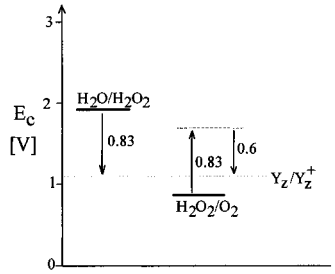

Figure 8. Hypothetical $2e^-/2e^-$ pathway for water oxidation. By stabilizing the intermediate (H_2O_2) by 0.83 eV and the product (O_2) by 0.6 eV by binding of the respective species to the Mn cluster, the potential for both oxidation steps can be reduced to the value of the couple Y_z/Y_z^+. The release of O_2 would be endergonic by 0.6 eV/molecule.

temperature dependence of the $S_3 \rightarrow S_4 \rightarrow S_0$ reaction is only 20 kJ/mol ($T > 279$ K), indicating that a large binding energy for O_2 is not present.

In a hypothetical, sequential $2e^-/2e^-$ oxidation scheme, the first reaction, $2H_2O \rightarrow H_2O_2 + 2H^+ + 2e^-$, has a configurational potential of $E_c = 1.931$ V. In order to reduce the potential of this reaction to that of Y_z at 1.1 V, the reaction product H_2O_2 is assumed to be stabilized by binding to the Mn site with a binding energy of 0.83 V (Figure 8). This would in turn raise the potential for the second reaction $H_2O_2 \rightarrow O_2 + 2H^+ + 2e^-$ (with released dioxygen) from $E_c = 0.870$ to 1.7 V. Allowing the dioxygen to be stabilized by 0.6 eV binding energy reduces the potential to 1.1 V. The release of dioxygen would then be uphill by 0.6 eV. In any case, the net energy difference between free reactants (H_2O) and free product (O_2) will always be the same and is determined by their free energies.

$^1H \rightarrow {}^2H$ isotopic analysis of the water oxidation reaction should provide important clues about the involvment of O-H bond cleavage in the rate-limiting step. However, an early study of the dependence of the kinetics of the various S state transitions on deuterium isotope substitution of water revealed only small effects.[77]

B. Predictions from Electronic Structure Calculations

The extended Hückel method has been used to calculate the relative energies of intermediates that might form during oxidation of water bound to μ-oxo bridged binuclear and tetranuclear Mn clusters of known geometry.[74] This approach does not offer a critical evaluation of the likely mechanism, it only compares the energetics along preselected reaction coordinates. Although the absolute values of energy differences in such calculations are questionable, some comparative conclusions could be drawn. Assuming equal O−O bond lengths, the formation of in-plane coordinated peroxide (type I, Figure 9) is predicted to be favored over the formation of out-of-plane (type II, Figure 9) coordinated peroxide, largely due to the stronger Mn−O π bonding permitted for the planar vs bent Mn_2O_2 rhombus. As Nishida pointed out,[78] type I coordination is predicted to lead principally to formation of singlet dioxygen product owing to ligand-to-metal charge transfer (Figure 9). Type II coordination, in contrast, leads to triplet (ground state) dioxygen. The additional energy

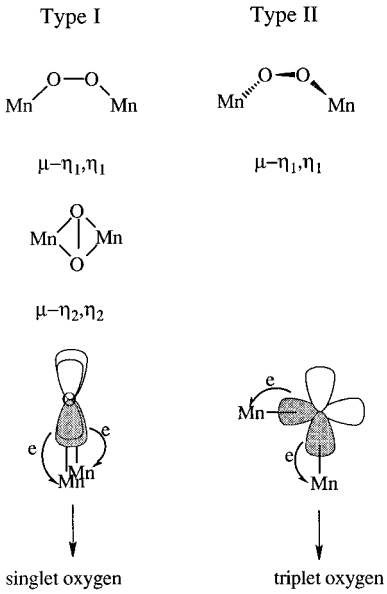

Figure 9. Two possible coordination modes of peroxide to a binuclear Mn complex: type I (in-plane) and type II (out-of-plane) coordination. Peroxide-to-metal charge transfer leads to the formation of singlet and triplet oxygen from type I and type II coordination, respectively.

required for singlet dioxygen formation is about 1 eV and should contribute to the barrier for dioxygen formation at type I centers. This may be compensated for in part if stronger binding occurs to Mn for type I vs type II coordination. An additional advantage for tetranuclear catalytic sites over binuclear sites was found to be a lower activation barrier to O−O bond formation due to greater charge delocalization.

The computational method was refined in a later study by Proserpio et al.,[4] adding a force-field calculation to optimize the geometries. For two different peroxo-bridged tetranuclear Mn clusters, a constrained minimization starting with type II (μ-η_1,η_1) peroxide coordination yielded a torsion angle of ~58°. The resulting activation barrier for O−O bond formation came out essentially equal to the previous study using an unrelaxed symmetrical type I (μ-η_2,η_2) coordinated peroxide (D_{2h} geometry) but about 1 eV lower than in (μ-η_1,η_1) (C_{2v}) geometry. Terminal rather than bridging hydroxo groups are used to form the O−O bond in the proposed mechanism, because the geometries suggested in the prior study (μ-η_2,η_2) (C_{2v}, D_{2h}) do not represent minimum energy structures according to the force-field calculation.

In conclusion, calculations suggest that oxidation of water to peroxide bound to four metal centers seems to decrease the energy barrier relative to coordination to a binuclear center, as might have been anticipated on the basis of elementary considerations of resonance interactions. The second step, oxidation of peroxide to dioxygen also is calculated to be easier in tetranuclear vs binuclear clusters, for the same reasoning.

V. Kinetics of Photosynthetic Water Oxidation

Thermodynamics tells one which reaction pathways are possible from an energetic standpoint. But exergonic reactions do not necessarily proceed at

observable rates. The importance of kinetic limitations against oxidation of water are found, for example, with Ce(IV) or MnO_4^- ions, which are both thermodynamically capable of oxidizing water in aqueous solutions, yet are, practically speaking, oxidatively inert owing to large activation barriers. Since it is the purpose of the catalyst to lower this barrier, it is instructive to look at the main contributions to the activation energy and how a catalyst could lower these.

There are two main contributions to the activation barrier.[66,75,79] The first is the energy of mutual approach of the oxygen atoms to form an O−O bond. The bond lengths of O_2 (0.121 nm) and H_2O_2 (0.145 nm) are considerably shorter than the sum of the van der Waals radii of two oxygen atoms (0.28 nm). The repulsion between the two oxygen atoms can be reduced by charge transfer from oxygen to metal ions in high oxidation states. Good examples are provided by bridging and terminal oxo groups (M−O−M, M═O) with both σ- and π-electron donation into empty or partially filled metal d-orbitals that lower the charge on oxygen. The only two structurally characterized homogeneous water-oxidation catalysts (vide infra) are known to form M═O bonds in their highest oxidation states. Thus, the metallo-oxene group seems to be a key feature for lowering the activation energy for O−O bond formation. However, as the example of $[(bpy)_2Ru^{VI}(O)_2]^{2+}$ and $[(bpy)_2Ru^{IV}(py)(O)]^{2+}$ shows (vide infra), the presence of metallo-oxene groups and a sufficient redox potential alone are not sufficient to fulfill the requirements for the oxidation of water. One could thus speculate that bridging oxo groups are important as well. On the other hand, there is no evidence for the involvement of the bridging oxo group in water oxidation by binuclear Ru−O−Ru complexes.

The second main contribution to the activation barrier to O−O bond formation is the reorganization energy of electron transfer, which—according to Marcus—can be divided into an inner sphere (change of bond lengths and angles) and an outer sphere part [change in polarization of the surrounding medium (solvent or protein)]. The fact that the outer sphere part is proportional to the square of the transferred charge[80] contributes to the unfavorability of the four-electron oxidation of water.

The outer sphere reorganization energy can be minimized by performing the electron transfer step in a medium with lower dielectric constant than water, i.e., a hydrophobic protein environment. The inner sphere part of the energy can be reduced by delocalization of charge by choice of large atomic radii or a multicenter catalyst.[66] A distorted nonequilibrium structure of the oxidized metal cluster, preorganized for O−O bond formation, a so-called "entactic state", would also offer a means for lowering the activation barrier.

In conclusion, stepwise electron transfer steps should have lower activation barriers than multi-electron transfer steps (assuming equal thermodynamic barriers!), and coupled proton−electron transfer steps which produce the least degree of charge separation are even more favored. The kinetic and thermodynamic feasibility of the oxidation of water to dioxygen therefore shows opposite trends. Therefore, as Krishtalik pointed out,[79] a $2e^-/2e^-$ pathway or a $2e^-/1e^-/1e^-$ pathway represent compromises between thermodynamic and kinetic constraints and hence could be favored over the thermodynamically most favored $4e^-$ pathway.

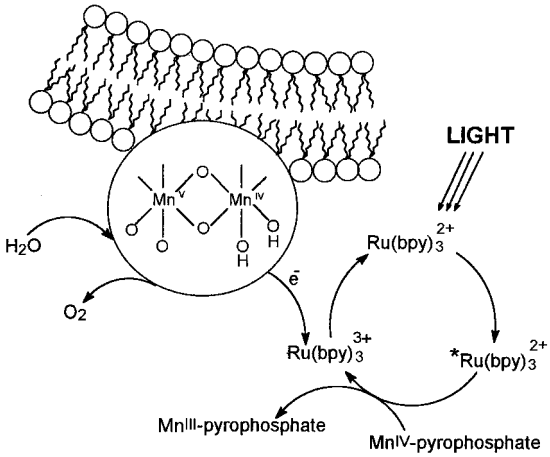

Figure 10. Catalytic system for the oxidation of water by Mn−oxo clusters, incorporated into phospholipid vesicles.[6]

VI. Mn–Oxo Clusters and Other Metal–Hydroxo Clusters as Catalysts[27]

MnO_2(s) and Mn_2O_3(s) are Mn(IV) and Mn(III) network polymers having the rutile structure and either the spinel structure (γ-type) or a structure with distorted hexacoordinated Mn (α-type), respectively. These materials are not active as water-oxidation catalysts without disruption of the solid structures as in colloids or freshly precipitated (hydrated) manganese (hydr)oxides. The reduction potentials of the oxides to form Mn(II) are 0.6 and 0.2 V, respectively, which are insufficient for water oxidation. This illustrates the strong stabilizing influence of oxide ligands and why the photosynthetic WOC must exclude access of too much water.

Shilov's group has shown since 1968 that colloidal MnO_2(s) catalyzes the oxidation of water to dioxygen in the presence of strong oxidants like Ce(IV), permanganate, $Ru(bpy)_3^{3+}$ and $Fe(bpy)_3^{3+}$ (ref 81). They have also shown that incorporation of Mn ions into phospholipid membranes leads to higher catalytic activities.[6,82] The catalyst was prepared by ultrasonic dispersion of dipalmitoylphosphatidylcholine in the presence of $MnCl_2$. It was found that Mn(II) was air-oxidized to Mn(III), which was tightly adsorbed on the lipid surface. Addition of 1 equiv of oxidant led to oxidation to Mn(IV) without oxidation of water. After further addition of oxidant, dioxygen evolved with higher yield than in heterogeneous suspensions of MnO_2. The involvement of Mn(V) intermediates in the catalytic reaction was therefore proposed. When $Ru(bpy)_3^{3+}$ was used as the oxidant, the dioxygen yield approached 65% based on the oxidant. An additional 20% was presumably consumed in the oxidation of Mn(III) to Mn(IV). A photocatalytic system was formed with $Ru(bpy)_3^{2+}$ as the photosensitizer and manganese(IV) pyrophosphate as the electron acceptor (Figure 10). The quantum yield for dioxygen production at neutral pH (Φ = 0.18) ap-

proaches that of the formation of $Ru(bpy)_3^{3+}$ in the absence of the catalyst ($\Phi = 0.25$). The dioxygen yield was 30% based on reduction of the electron acceptor manganese(IV) pyrophosphate.

The authors stressed the implications of these experiments on the mechanism of the evolution of the water-oxidation catalyst in Nature.[83] In comparative studies using low oxidation state 3d metal salts, it was shown that Mn was the most effective catalyst in water oxidation in the vesicular system. Moreover, in contrast to Mn(IV) clusters, RuO_2 oxidizes the lipids rather than water in this system.

The cluster size was proposed to be further reduced by using cyclodextrins as a stabilizer for Mn−oxo clusters.[84] The catalysts were prepared by ultrasonic dispersion of cyclodextrins in the presence of Mn(II) salts. The dioxygen yield using $Ru(bpy)_3^{3+}$ as the oxidant approached 80% and was strongly dependent on the pH, peaking at pH 7. A redox-active dimanganese(II,II)−β-cyclodextrin complex has been previously characterized in solution.[85]

In other experiments[86,87] Mn(III) and Co(III) complexes were hydrolyzed in the presence of polyvinyl alcohol or starch as stabilizers for preparing colloidal solutions of metal hydroxides and were used as water oxidation catalysts. The reactivity of analogously prepared samples varied significantly, indicating the poor reproducibility of these experiments.

These studies suggested an increased activity of metal hydroxo clusters as catalysts for water oxidation with decreasing cluster size. In none of the experiments could the cluster size be determined reliably.

VII. Water Oxidation by Discrete Manganese Complexes

Although manganese is the essential cofactor that Nature employs for the catalytic oxidation of water in photosystem II, there are only a few reports of synthetic manganese compounds which are able to catalyze this reaction. Moreover, most of them act in a noncatalytic fashion, and those which do act catalytically are most often structurally undefined solids. However, knowledge of those compounds which do perform the reaction in some way might help in pointing out some common features which must be included in the strategy to synthesize more well-defined and more effective catalysts in the future.

It was recognized back in 1913[88] that aqueous permanganate liberates dioxygen upon irradiation in aqueous solution. A detailed study in 1955 by Zimmerman[41] attempted to reveal the mechanism of this reaction by measuring its dependence on the wavelength of the incident light, pH (6.8−13), temperature, and the isotopic composition of the medium. The results showed that mainly the UV absorption band around 310 nm is active in the photodecomposition reaction. Isotopic labeling of the solvent water showed that both oxygen atoms come from permanganate. A mechanism could not be deduced from the data. A more recent study was conducted by Lee et al.[7] The reaction proceeds by direct formation of MnO_2^- and O_2 as the reaction products at acidic pH. At neutral or basic pH, MnO_2 and MnO_4^{2-} are formed, respectively, besides O_2, by subsequent reaction of the initial reaction product MnO_2^-. Addition of an oxidizable substrate (like acetone) to the photolyzed permanganate solution produced an interesting result: the rate of decomposition of permanganate increases while the dioxygen yield decreases. This was interpreted by the mechanism shown in Scheme 3. It was concluded that a long-lived intermediate (**I**) exists, which is common to both reactions, dioxygen evolution and substrate oxidation. By addition of an oxidizable substrate, the intermediate is trapped, thus reducing the dioxygen yield while accelerating permanganate decomposition. In analogy with other metal−peroxo complexes, the intermediate was proposed to be the manganate(V)−peroxo species shown in Figure 11. Its long lifetime was explained by proposing a high activation barrier to the symmetry-forbidden (Woodward−Hoffman rules) thermal back-reaction to permanganate. Photoexcitation in the 310 nm band system and the visible band system are assigned to $O(\sigma) \rightarrow Mn(d_z^2)$ LMCT and $O(\pi) \rightarrow Mn(d_z^2)$ LMCT one-electron charge transfer transitions, both yielding $^1B_2$ excited states. These correlate smoothly with corresponding states in the lower C_{2v} symmetry of the proposed intermediate. Direct or thermally assisted vibronic coupling, respectively, was proposed to enable transfer of the remaining electron from the same ligand orbital to the Mn ion, yielding Mn(V) and peroxo. Because this corresponds to a two-electron excited state of the same symmetry as the ground $^1A_1$ state, an avoided crossing occurs. This provides an explanation for both a long-lived intermediate in the photochemical mechanism and the high thermal barrier to decomposition in the ground state.

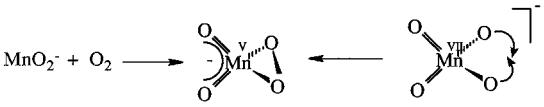

Figure 11. Possible formation of a Mn(V)−peroxo species as an intermediate in permanganate photodecomposition.[7]

Scheme 3. Pathways for the Photochemical Decomposition of Permanganate[7]

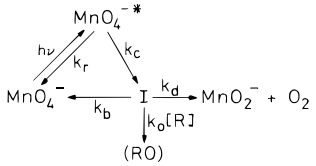

One of the best studied dimanganese complexes is $[(bpy)_2Mn^{III}(\mu\text{-}O)_2Mn^{IV}(bpy)_2]^{3+}$. Its functionality as a water-oxidation catalyst was studied as well. The redox potential of $[Mn^{IV}{}_2L_4(O)_2]^{4+} + e^- \leftrightarrow [Mn^{III}Mn^{IV}L_4(O)_2]^{3+}$ (L = bpy, phen) is sufficient to oxidize water to dioxygen via a four-electron reaction. The oxidation of water was not observed in homogeneous aqueous solution with Ce(IV) added as an oxidizer.[89] However, when solid material was present in a saturated solution or the complex was absorbed into kaolin clay,[90] dioxygen evolved from the solid with low yield. Isotopic labeling of the solvent water showed that indeed water was oxidized. The decomposition product after completion of the reaction was identified as MnO_4^- by its UV spectrum. When the complexes were incorporated into a Nafion film coating a BPG (basal plane graphite) electrode, higher

cathodic currents were recorded.[91] The manganese complexes were obviously acting as redox mediators.

Similar behavior was observed with a Schiff base complex. When $(NH_4)_2Ce(SO_4)_3$ is added to a saturated aqueous solution of the complex $[Mn(salen)(H_2O)]_2(ClO_4)_2$, a brown precipitate forms and dioxygen evolves from this precipitate.[92] The evolved gas was analyzed by GC to consist of both O_2 and N_2, the latter presumably by oxidation of NH_4^+. The turnover number was 10−13 for O_2/N_2 evolution. Absorbing the complex on kaolin clay or incorporating it into a Nafion-coated electrode yields similar results as seen with the bpy dimer (vide supra). These results suggest that the observed behavior of the complexes is independent of the starting material. The catalytic activity is, much like above, most likely attributable to an oxidized hydrolysis product of the complexes, rather than the complexes themselves.

The photochemistry of the above Mn−bpy dimers was investigated by Otsuji et al.[93] The (III,IV) oxidation state of the complexes is thermodynamically not able to oxidize water. Upon irradiation in acidic solution (H_2SO_4, H_3PO_4; $[H^+] \sim 0.05-0.5$ M) with light of the wavelength 300 nm $< \lambda <$ 320 nm, H_2O_2 was detected by polarographic measurements together with formation of Mn(II). The initial formation of hydroxyl radicals by photoreduction of the (III,IV) to the (III,III) complex was proposed, since addition of phenylacetic acid led to the formation of benzyl alcohol. The hydroxyl radicals could dimerize to form H_2O_2. However, recent results indicate that the observed photochemistry is not attributable to the Mn−bpy (III,IV) dimer. It is known that the Mn−bpy dimer disproportionates rapidly at low pH upon protonation of the μ-oxo group (pK = 2.3 (ref 94)) and products of higher nuclearity form in strongly acidic solution.[95,96] In H_3PO_4, a Mn(IV,IV) dimer is formed by disproportionation and stabilized by phosphate.[97] The observed photochemistry is still interesting and it would be worth knowing what the reactive species is and how the reaction proceeds mechanistically.

Boucher and Coe reported in 1975[8] that hydrogen peroxide was produced [detected by using an iron(II) thiocyanate solution] when $HClO_4$ was added in stoichiometric amounts to solutions of the Mn(IV) Schiff base dimer $[Mn^{IV}_2(BuSalen)_2(O)_2]\cdot H_2O$ in acetone at 0 °C. [There is no evidence that the complex remains dimeric in acetone solution.] The complex was converted in 62% yield to the Mn(III) monomer $[Mn(BuSalen)(H_2O)]ClO_4$ from which the dimer was initially synthesized by air oxidation in chloroform solution (Figure 12). The authors proposed that the doubly protonated Mn^{IV}_2−bis-μ-hydroxo complex is an intermediate in the reaction. Interestingly, the reaction sequence leads formally to the following equation

$$2H^+ + 2OH^- + {}^1/_2O_2 \rightarrow H_2O_2 + H_2O \qquad (5)$$

which would be the catalytic oxidation of water to H_2O_2, using dioxygen.

This report provided the first evidence for the formation of H_2O_2, presumably by coupling of bridging oxos in a Mn dimer. However, since the chemical detection method for peroxide is rather unspecific (all species which oxidize the Fe(II) complex are detected), the actual presence of peroxide might be doubtful. Moreover, dioxygen evolution could not be detected. This is surprising since Pecoraro later found catalase activity for a similar Mn(IV) dimer with salpn as the ligand.[26] Thus, excess Mn(IV) dimer should have dismutated the peroxide product to yield dioxygen.

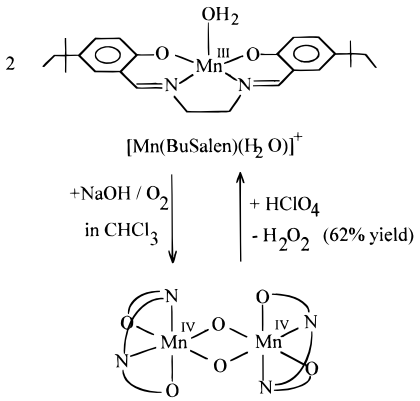

Figure 12. The synthesis and decomposition of a Mn(IV) Schiff base dimer leads formally to the oxidation of water to hydrogen peroxide with oxygen.[8]

The reverse reaction, the reduction of dioxygen to H_2O_2, was observed by Kitajima et al.[98] It was observed that $[Mn^{II}_2(OH)_2L_2]$ [L = HB(3,5-iPr_2pz)$_3$; see Figure 13] is oxidized by air to a mixture of $[Mn^{III}_2(O)_2L_2]$ and $[Mn^{III}_2(O)L'_2]$ where L′ is the ligand L with one i-Pr group hydroxlyated at C-2. For the latter species, isotopic labeling proved that both hydroxyl groups on the ligand came from O_2, while the μ-O groups are retained from the starting complex. This led to a proposed reaction scheme with a μ-peroxo complex as the common intermediate that could decompose by either of the two competing pathways (Figure 13). The novel feature of the peroxide elimination pathway is that the reverse reaction utilizes the $Mn^{III}_2(\mu\text{-}O)_2$ core as both an oxidant and as proton acceptor for conversion of peroxide to O_2. This is a clear example of the coupling of proton and electron transfer steps.

Mn(IV) Schiff base monomers were found to oxidize water to molecular oxygen in acetonitrile/water solution.[10,11] The formulation of the complexes as *trans*-$Mn^{IV}L_2Cl_2$ (L = *N*-alkyl-3-nitrosalicylimide) (Figure 14) was supported by elemental analysis, magnetic susceptibility, IR, and UV−vis spectral data. Cyclic voltammetry in acetonitrile showed two reduction waves at 0.96−1.04 V and 0−0.28 V, varying with the alkyl residue.

Dioxygen evolution was monitored by an oxygen electrode as well as with pyrogallol solution. A maximum of 0.27 mol of O_2 per mol of complex was detected at neutral pH (phosphate buffer) which is about 50% of what is expected by the equation shown below. Two chloride ions were released per Mn complex as determined by titration with $AgNO_3$. The reaction product was isolated and identified as $Mn^{II}L_2(H_2O)_2$ (L = *N*-propyl-3-nitrosalicylimide) by its elemental analysis, electronic and IR spectra, and magnetic susceptibility. Thus the reaction can be formulated as

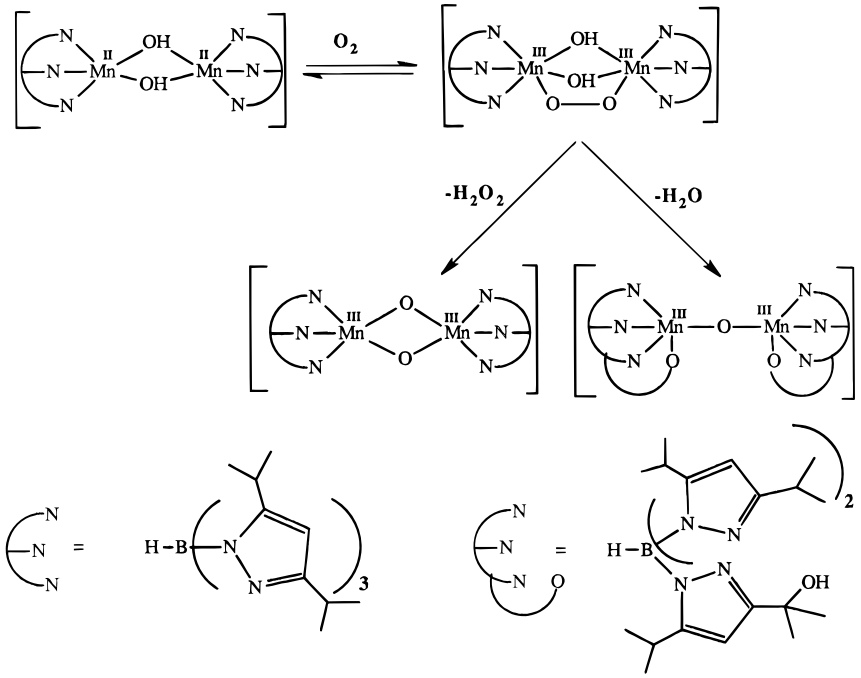

Figure 13. Proposed reduction of oxygen to hydrogen peroxide and observed hydroxylation of the ligand with a dimanganese complex.[9]

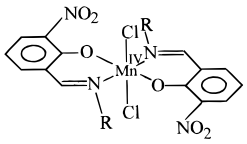

Figure 14. Proposed structure of the complex *trans*-$Mn^{IV}L_2Cl_2$ (L = *N*-alkyl-3-nitrosalicylimide) implicated in water oxidation.[10,11]

$$2Mn^{IV}L_2Cl_2 + 4H_2O \rightarrow 2Mn^{II}L_2(H_2O)_2 + O_2 + 4H^+ + 4Cl^- \quad (6)$$

Even though the Mn(IV) complexes are mononuclear, a binuclear step in the mechanism can be anticipated, since the overall reaction involves the transfer of four electrons. The O−O bond formation could be either inter- or intramolecular with a bound η_1,η_1-peroxide as an intermediate in the latter case. The reactivity of the complexes decreased with the length of the alkyl chain attached to the imine nitrogen. Using ^{18}O-labeled water showed that indeed water was oxidized. This reaction suggests that chloride, a functionally required anion for photosynthetic water oxidation, can serve to maintain a high oxidation potential of the Mn(IV) ions, so that upon exchange with water ligands intramolecular oxidation of water and reduction of Mn(IV) can proceed. This theme has been previously supported by electrochemical studies.[99]

Ashmawy and co-workers observed dioxygen evolution from Mn(III) Schiff base complexes of the type $\{[Mn^{III}L(H_2O)]_2\}^{2+}$ (L = salen [$(CH_2)_2$], salpd (saltm) [$(CH_2)_3$], salbd [$(CH_2)_4$], salpn [(CH_2CHMe)], salphen [o-C_6H_4], 3,5-dichloro-salen) upon irradiation in the presence of quinones in aqueous or ethanol solution.[100−102] A precipitate formed during the noncatalytic reaction. The solid state structures of the complexes were shown to be dimeric (crystal structures) for $[Mn(3,5\text{-diclorosalen})(H_2O)_2]_2(ClO_4)_2$[102] and

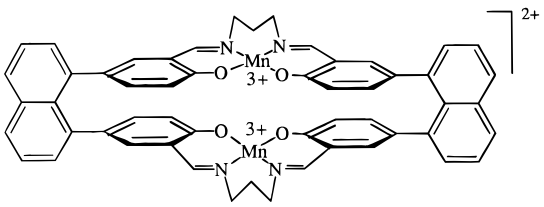

Figure 15. Proposed structure of a Mn Schiff base dimer implicated in photolytic water oxidation.[12]

$[Mn(salen)(H_2O)]_2(ClO_4)$[103] with bridging water molecules only in the former case and a semibridging phenoxy group in the latter. This contradicts the proposition by the authors that the dioxygen might stem from bridging water molecules. While the complexes are monomeric in acetone, conductivity measurements indicated a monomer in equilibrium with a aquo-bridged dimer in aqueous solution. The wavelength dependence of the reaction rate shows a maximum for photolysis in the 450−600 nm region, where the quinone does not absorb. Interestingly, all complexes which showed photolytic activity had an absorption band at 590 nm and the complex with the highest extinction coefficient for this band, $[Mn(saltm)(H_2O)]^+$, showed the highest activity. Recently, another Mn Schiff, base dimer with a covalent dinuclating ligand was reported to exhibit photolytic activity for dioxygen evolution[12] (Figure 15). This compound seems to have rather different geometry than the dimers shown above. This shows that the photolytic activity is rather structure unspecific.

Recently, the first structurally characterized and truly catalytic manganese water oxidation catalyst was reported.[13] It was shown that a *o*-phenylene-bridged Mn(III)−phorphyrin dimer (Figure 16) is capable of catalyzing the electrochemical oxidation of water at potentials above 1.2 V (vs Ag/Ag^+) in a mixed acetonitrile/water (95/5) solvent containing n-Bu_4NOH as the supporting electrolyte. The Faradaic efficiency was 5−17% in the range of 1.2 to 2 V

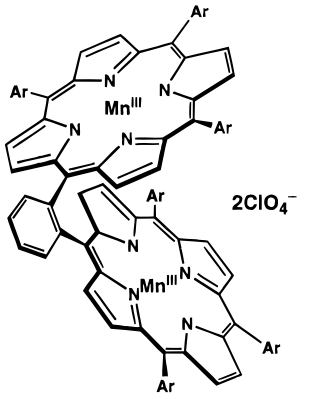

1 Ar = 4-*t*-BuC$_6$H$_4$

2 Ar = 2,4,6-Me$_3$C$_6$H$_2$

3 Ar = C$_6$F$_5$

Figure 16. Structure of an *o*-phenylene-bridged Mn−porphyrin dimer which was used as a electrocatalyst for the oxidation of water. Reprinted from ref 13; copyright 1994 VCH.

anodic potential. The turnover number for the most active species was 9.2, the rate of dioxygen evolution being first-order with respect to the complex (maximum rate = 0.11 [cat.] min^{-1} at 2.0 V). When isotopically labeled water was used, the evolved dioxygen had the expected statistical isotope distribution, showing that the dioxygen stems from solvent water. The complexes showed no catalase activity, and free H_2O_2 was not produced during the reaction. The number of electrons involved in the reaction was determined with a rotating disk electrode to be 3.7. Thus, a four-electron mechanism seems likely, although there is no proof of the mechanism. It can be speculated that Mn(V)=O groups are intermediates in the reaction. Two pathways, either direct coupling of neighboring manganoyl-oxo groups or solvent attack on one Mn=O group and oxidation of the resulting peroxointermediate, can be envisioned. Further studies are needed to confirm either of these possibilities.

An interesting class of heterogeneous catalysts was introduced recently.[14] The silsesquioxanes, synthesized from phenyltrichlorosilan by hydrolysis, contain a 12-membered ring of Si and O atoms. The corresponding hexasodium salt reacts with various transition metal chlorides to give "sandwiched" hexanuclear ring structures with the metal ions being ligated by four μ_2-siloxy groups forming a ring of three dimers of the type (M(μ-OR)$_2$M(μ-OR)$_2$)$_3$. A terminal water ligand on each metal ion and a μ_6-chloride ion in the center of the structure complete the ligation shells (Figure 17). Since these compounds are water-insoluble, they were supported on soot (C), SiO_2, or γ-Al_2O_3. Oxidation of a suspension of these materials with Ru(bpy)$_3^{3+}$ led to evolution of dioxygen with the Fe_6 and Mn_6 complexes. The yield of dioxygen, based on the oxidant, varied between the different supports. The highest yields were achieved on soot, with 55% for the Fe_6 and 17% for the Mn_6 species.

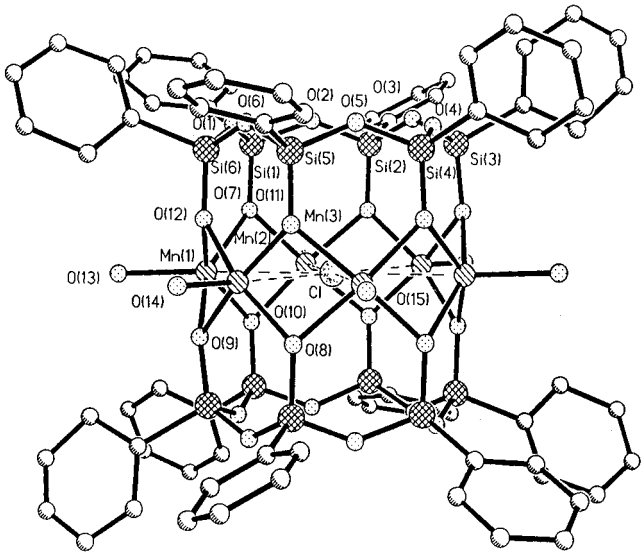

Figure 17. Crystal structure of a Mn (or Fe) silsesquioxane hexanuclear complex which is a heterogeneous catalyst for the oxidation of water to oxygen. Reprinted from ref 14; copyright 1994 Elsevier.

VIII. Water Oxidation by the Ru Dimer [(bpy)$_2$(H$_2$O)RuORu(H$_2$O)(bpy)$_2$]$^{4+}$

A. Redox and Protonation Equilibria

There is an extensive chemistry developed for high oxidation state Ru compounds containing polypyridyl ligands. Mononuclear complexes like [(bpy)$_2$Ru^{II}(py)(H$_2$O)]$^{2+}$ or [(bpy)$_2$Ru^{II}(H$_2$O)$_2$]$^{2+}$ can undergo reversible two- and four-electron oxidations forming Ru(IV) and Ru(VI), respectively. A variety of organic and inorganic substrates can be oxidized with this system.[104] However, the demands for the four-electron oxidation of water could not be met with these complexes. The reasons for this are unclear. For the latter complex, bpy ligand dissociation leads to catalyst degradation and loss of water oxidation capability.

In 1982, Meyer's group reported the catalytic oxidation of water and chloride with a binuclear Ru complex [(bpy)$_2$(H$_2$O)RuORu(H$_2$O)(bpy)$_2$]$^{4+}$ (**1**).[105] The stability of the catalyst, however, is limited to 10−25 turnovers by oxidative degradation and water−anion ligand exchange of the catalyst. Since then, complex (**1**) and related compounds have been extensively studied in order to elucidate the mechanism of water oxidation and increase the efficiency and stability of the catalyst.

The crystal structure of (**1**) is shown in Figure 18.[15] The two Ru(III) centers are approximately octahedrally coordinated. The Ru−O−Ru angle approaches linear at 165.4°. The two aquo-ligands are straddled, occupying gauche positions to each other with a dihedral angle of 65.7°. Molecular mechanics calculations on the dimer, however, show that the barrier for rotation around the Ru−O bonds is small, so that the solution conformation should be dynamic.[16]

Compound (**1**) exhibits a rich redox chemistry, coupled with acid−base equilibria of the aquo ligands. The redox potentials are therefore pH-dependent. These equilibria are summarized best in a plot of the reduction potential vs pH or Pourbaix diagram, shown in Figure 19.[15,104] The pK_a values of the aquo ligands are indicated as vertical lines. They are 5.9

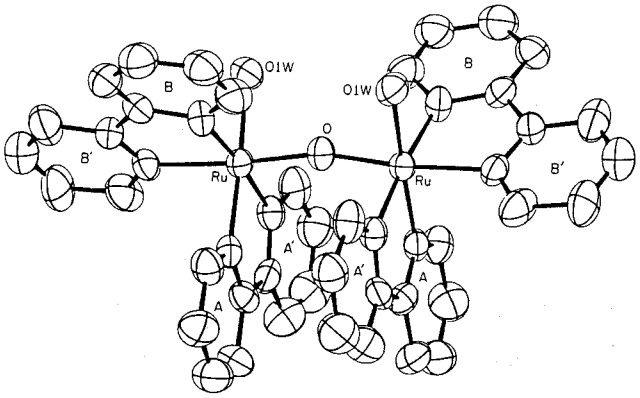

Figure 18. Crystal structure of $[(bpy)_2(H_2O)Ru^{III}ORu^{III}(H_2O)(bpy)_2]^{4+}$ reprinted from ref 15; copyright 1985 American Chemical Society.

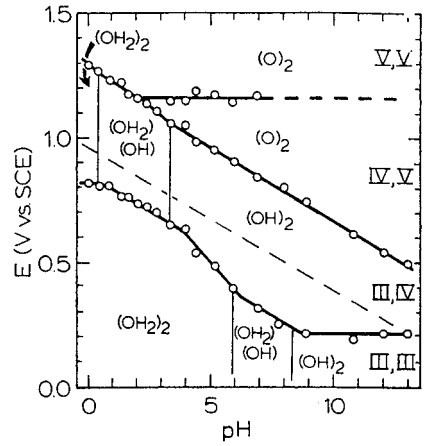

Figure 19. Electrochemical potential vs pH diagram for the Ru dimer (**1**). Reprinted from ref 15; copyright 1985 American Chemical Society.

and 8.3 for the (III,III) and 0.4 and 3.3 for the (III,-IV) forms, as determined by titration[15] and confirmed by resonance Raman studies.[106] A few general features can be extracted from Figure 19:

1. The one-electron oxidation of the (III,III) to the (III,IV) species can be described by five distinct reactions as a function of pH, according to the number of protons taken up or released to solution. Reactions with zero, one, or two protons have been observed.

2. Further oxidation of the (III,IV) species can occur either as a three-electron process or a two-electron process, depending on the pH. In the latter case another one-electron process at higher potential leads to the (V,V) state. The (IV,IV) species is apparently unstable over the whole pH range and is not detected by electrochemical measurements (Ramaraj et al. claimed that the redox reactions for (**1**) are (III,III) ↔ (IV,IV) ↔ (V,V), as seen by CV. However, his evidence identifying the (IV,IV) species is weak.)[107] In addition, according to electrochemical data of Gilbert et al., the (IV,V) form is unstable with respect to disproportionation below pH 2.2. This was later contradicted by Hurst et al. who showed RR and EPR evidence for the formation of the (IV,V) state at pH 1. The redox reactions can therefore be written as:

$$(III,III) \xleftrightarrow{1e^-} (III,IV) \xleftrightarrow{3e^-} (V,V)$$

$$(III,III) \xleftrightarrow{1e^-} (III,IV) \xleftrightarrow{2e^-} (IV,V) \xleftrightarrow{1e^-} (V,V)$$

(the proton transfer depends on the pH and is omitted here).

3. The (V,V) state has the terminal aquo ligands fully deprotonated at all pH (Ru=O). This was confirmed by resonance Raman studies.[106] However, there is evidence that the bridging μ-oxo group might get protonated in strong acids.[108]

Some of the oxidation steps in the cyclic voltammetry experiments were irreversible or quasi-reversible due to complex electrode reaction kinetics and water oxidation catalysis. The assignment of the higher oxidation states, especially the (V,V) state, could therefore not be confirmed by coulometry. It is noteworthy that the occurrence of oxidations states as high as (V,V) in the cyclic voltammogram of (**1**) is only due to the fact that it is a sluggish catalyst for the oxidation of water. Related Ru complexes which show faster water-oxidation kinetics do not allow detection of such high oxidation states (vide infra).

In addition to the metal-centered oxidation states that were proposed on the basis of electrochemical studies, EPR studies[108] indicate that a ligand-based oxidation state, involving a bipyridyl-centered radical derived from (**1**) could be present in strongly acidic solutions containing strong oxidants. The oxidation of complex (**1**) with Ce^{4+} in 1 M triflic acid produced a nearly isotropic $g = 1.95$ signal of 40 G width which persisted to temperatures as low as 5 K. In comparison with ligand radicals of $Ru(bpy)_3^{-/0/+}$, it was tentatively assigned to a ligand π-radical of (**1**).

The aforementioned ligand oxidation is interesting, because a similar effect occurs upon calcium depletion of the WOC of PSII. An amino acid adjacent to the tetra-Mn cluster is stably photo-oxidized on the S_2' to S_3' transition, instead of transferring the oxidizing equivalent to Mn. There is recent evidence that the radical is Y_Z, the physiological electron carrier between Mn and the special chlorophyll P680.[49,50]

Knowledge of the redox potentials allows a thermodynamic analysis of the possible net reactions of water oxidation by different oxidation states of the dimer (**1**). Table 4 lists the driving force for several net reactions for the (V,V) and (IV,V) oxidation states at different pH values. The analysis shows that the (V,V) form strongly favors oxidation of water to dioxygen between pH 1 and 7 (eqs 1 and 2). Because the (V,V) form can act as a four-electron oxidant, dioxygen formation can be achieved, in principle, by one (V,V) ion. The formation of free intermediates like superoxide (eq 3) or hydroxyl (eq 4) radicals on the other hand constitutes nonspontaneous thermodynamically less favored reactions. The formation of OH radicals can be excluded. However, the formation of HO_2 or H_2O_2 as bound or free intermediates is plausible, since it could be the slowest step, followed by a fast subsequent oxidation to O_2.[15] A calculation of the lower limit of the rate constant, obtained by using the free energy change as the lower limit to the activation barrier, reveals that a rate in the seconds time scale for the water-oxidation reaction could be achieved even if the mechanism were to include such an uphill step. The (IV,V) form is

Table 4. Thermodynamic Driving Force of Various Net Reactions of Water Oxidation by Ru Dimer $[(bpy)_2(H_2O)RuORu(H_2O)(bpy)_2]^{3+}$ [15]

no.	pH	reaction	$\Delta G^{\circ\prime}$ (ev)
1	1	$[(O)Ru^{V}ORu^{V}(O)]^{4+} + 2H_2O \rightarrow O_2 + [(H_2O)Ru^{III}ORu^{III}(H_2O)]^{4+}$	−0.72
2	7	$[(O)Ru^{V}ORu^{V}(O)]^{4+} + 2H_2O \rightarrow O_2 + H^+ + [(OH)Ru^{III}ORu^{III}(H_2O)]^{3+}$	−0.80
3	1	$[(O)Ru^{V}ORu^{V}(O)]^{4+} + 2H_2O \rightarrow HO_2 + [(H_2O)Ru^{III}ORu^{IV}(OH)]^{4+}$	0.45
4	3	$[(O)Ru^{V}ORu^{V}(O)]^{4+} + 2H_2O \rightarrow OH^{\bullet} + H^+ + [(O)Ru^{IV}ORu^{V}(O)]^{3+}$	1.2
5	7	$2[(O)Ru^{IV}ORu^{V}(O)]^{3+} + 2H_2O \rightarrow O_2 + 2\,[(OH)Ru^{III}ORu^{IV}(OH)]^{3+}$	−1.00
6	7	$[(O)Ru^{IV}ORu^{V}(O)]^{3+} + 2H_2O \rightarrow H_2O_2 + [(OH)Ru^{III}ORu^{IV}(OH)]^{3+}$	0.58

also thermodynamically capable of oxidizing water to dioxygen, even at pH 7 (eq 5). However, two Ru dimers are necessary for this reaction. This makes mechanistic studies comparing the (V,V) and the (IV,V) form interesting (vide infra). Again, formation of free (or bound) intermediates like peroxide is less favorable and constitutes an uphill reaction.

B. Isotope-Studies—Speculative Mechanisms

The mechanism of water oxidation by complex (**1**) was addressed by two isotopic labeling studies. Geselowitz and Meyer[109] found a ratio of 13% $^{18}O_2$, 64% $^{18}O^{16}O$, and 23% $^{16}O_2$ when the terminal aquo ligands were ^{18}O-labeled in the (III,III) or (III,IV) complex and then oxidized with 5 and 4 equiv of Ce(IV) in 0.1 M trifilic acid, respectively. Hurst et al.[106] addressed the problem again using fully labeled (III,-III) complex (oxo bridge + terminal aquo ligands) and oxidizing with 5−6 equiv of Co(III) in 1 M triflic acid. The dioxygen product contained roughly 50% $^{16}O_2$, with the remainder being $^{18}O^{16}O$. In contrast to the earlier study, there was no evidence for $^{18}O_2$ formation. This might be a result of the differing reaction conditions. On the other hand, even though the isotopic composition of the dioxygen did not change during the course of the reaction, fast isotopic scrambling cannot be excluded in either of these studies. The results suggest that direct coupling of Ru=O groups is unlikely, since it would lead primarily to doubly labeled dioxygen. On the other hand, solvent water attack on ruthenyl-oxo groups cannot be the only mechanism operating, because this would lead to singly labeled product. At least two separate mechanisms must be operative in order to account for the nonlabeled and mixed-labeled dioxygen. Otherwise, the results are inconclusive; neither intramolecular nor intermolecular processes could be eliminated.

Early speculations invoked reductive elimination of H_2O_2 or O_2 from the adjacent ruthenyl-oxo groups in the (V,V) oxidation state of the catalyst (Figure 20, top). This mechanism can be excluded on the basis of the labeling studies, as well as by the fact that asymmetric Ru dimers with one water ligand substituted by pyridine can evolve dioxygen from a (V,III) oxidation state[110] (there is ambiguity because it cannot be excluded that py is partially lost and replaced by water during the reaction). In addition, sterically constrained dimers using linked bpy−x−bpy ligands (vide infra), where close approach of the oxo groups is prohibited, also evolve O_2 by water oxidation. Dioxygen cannot be formed here through coupling of adjacent terminal Ru−oxo groups.

Meyer[104] proposed that the nonlabeled dioxygen could be formed after attack of solvent water on an initially formed dihydroozone intermediate, containing an (−HO−O−OH−) bridge (Figure 20, middle). Hurst et al.[106] accounted for the singly labeled dioxygen by formation of a speculative peroxo intermediate after solvent attack on a terminal Ru−oxo group, while the nonlabeled dioxygen was proposed to be formed from an intermediate formed by solvent attack on two adjacent terminal Ru−oxo groups (Figure 20, bottom).

The kinetics of water oxidation by complex (**1**) were investigated with two different approaches. First, the (IV,V) oxidation state was produced with a stoichiometric amount of oxidant and the initial rate of its decay followed by UV spectral changes. Second, the steady-state kinetics of water oxidation was investigated using excess oxidant and generating the (V,V) oxidation state.

The (IV,V) complex reverts to the (III,IV) oxidation state with slow evolution of dioxygen in ∼95% yield (it is about 100 times slower than with the (V,V) complex).[111] The observed rate law indicates that the rate-limiting step is unimolecular with respect to the (IV,V) complex and seems to be independent of pH between pH 2.5 and 10.8 in phosphate buffer. The rate constant is on the order 3×10^{-4} s^{-1}. Since the (IV,V) state is a two-electron oxidant, two catalyst molecules must be involved in the four-electron oxidation of water. A stepwise mechanism with formation of free or bound H_2O_2 as an intermediate can be anticipated, but was not be experimentally established.

Lei and Hurst[112] produced the (V,V) oxidation state at pH 0−1 in triflic acid, using excess Co(III)/Co(II) mixtures as the oxidant, and monitoring dioxygen evolution using a Clark-type electrode (method of initial rates). The reaction rate showed a first-order dependence on the initial catalyst concentration when the Co(III) and Co(II) concentrations were fixed. The dependence of the rate on the cobalt concentrations was complex and could be fit equally well to two different rate laws. The data analysis suggested that the (V,V) or a higher oxidation state (i.e. involving a ligand radical) is the active species, reverting either to the (III,III) state forming dioxygen directly or the unstable (IV,IV) state producing H_2O_2, which in turn is quickly oxidized to dioxygen by excess Co(III). Rate constants between 0.4 and 0.8 min^{-1} were calculated.

The kinetic studies show unimolecular mechanisms for the rate-limiting step. However, no further information about the mechanism could be established.

IX. Water Oxidation with Related Ru Complexes

In addition to the Ru dimer (**1**), a variety of related Ru complexes have been synthesized and proven to be active water-oxidation catalysts.

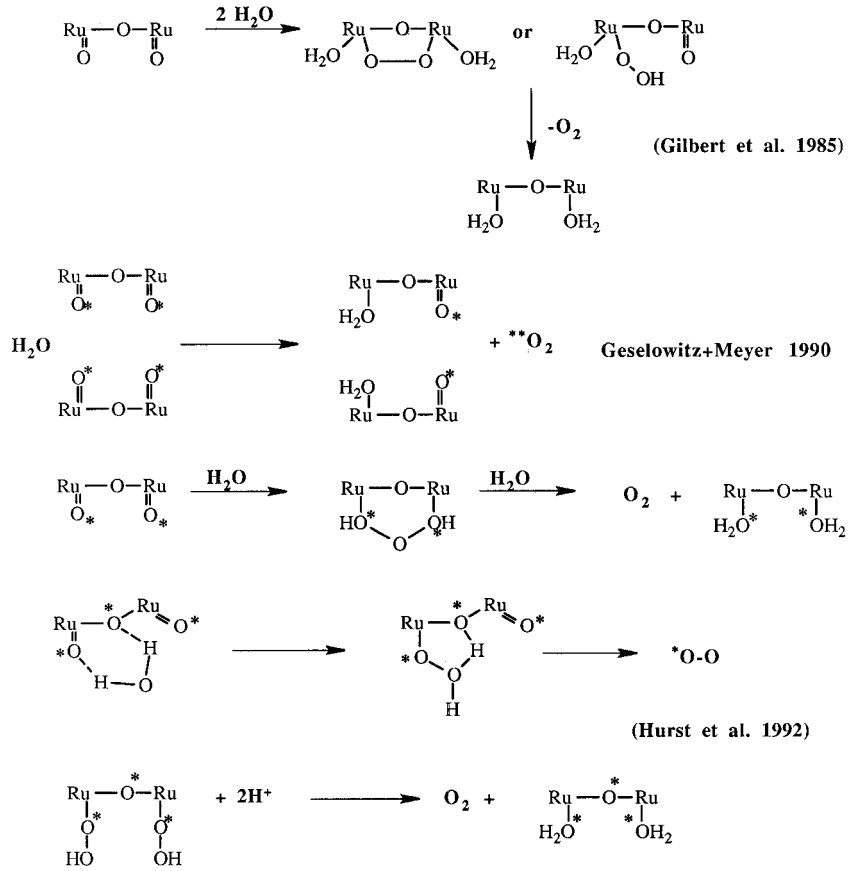

Figure 20. Mechanisms for the oxidation of water by (**1**) which cannot be excluded by available data (primarily ^{18}O-labeling studies).

Rotzinger et al.[113] studied the properties of a Ru dimer, substituting bpy-5,5′-dicarboxylic acid (L) for bpy. It was prepared by electrochemical oxidative dimerization of $Ru^{II}L_2(H_2O)_2^{2+}$ in 0.5 M H_2SO_4. The reduction potential for the (III,III)−(III,IV) couple lies at 0.98 V (vs SCE in 0.5 M H_2SO_4). Higher oxidation states could not be characterized, because catalytic water oxidation interfered above 1.1 V. This irreversibility shows that the catalytic process is much faster than with (**1**), for which CV revealed long-lived oxidation products on the time scale of 50 mV/s sweep rates. It implies a millisecond time scale for the water-oxidation reaction compared to seconds for (**1**). Using excess Ce(IV) as the oxidant, a turnover number of 75 could be achieved without catalyst degradation (vs a turnover number of ∼15 for (**1**)). Nazeeruddin et al.[114] found for the same catalyst that the (III,IV) oxidation state is able to oxidize water in a reaction with stoichiometry

$$4(III,IV) + 2H_2O \rightarrow 4(III,III) + O_2 + 4H^+$$

Disproportionation of the (III,IV) state to the (III,III) and (IV,IV) states is presumed to be the first step in the catalytic cycle. This is a remarkable difference vs the bpy complex (**1**), where at least the (IV,V) oxidation state is needed to achieve the oxidation of water. The driving force for water oxidation is extremely low, and the disproportionation to yield (IV,IV) is presumed to be nonspontaneous, by analogy to (**1**). Presumably, the lower net charge of the complex vs (**1**) reduces any electrostatic barrier to this bimolecular reaction, which may account for this new pathway.

In a similar manner, the Ru dimer with bpy-4,4′-dicarboxylic acid was synthesized and characterized by Comte et al.[115] The pK_a values of the terminal aquo ligands for the (III,III) oxidation state are similar to those of the bpy complex (6.2 ± 0.2 and 8.5 ± 0.4), as found by spectrophotometric titration. The reduction potential for the (III,III)/(III,IV) couple lies at 0.9 V (vs SCE) in 1 M triflic acid (quasi-reversible), while higher redox states could not be identified because of interference from catalytic water oxidation (vide supra). In contrast to the above mentioned complexes, reduction to the (II,II) species is reversible at pH 3.25. Water oxidation was induced by adding excess Co(III). The maximum turnover number was 33, while 40% of the catalyst was destroyed during the reaction. Therefore, this catalyst shows faster O_2 formation kinetics than (**1**), but lower stability than the 5,5′-dicarboxylate complex. In order to shed light on the mechanism of water oxidation, pulse radiolysis studies were conducted. The (III,IV) complex was oxidized to the (IV,IV) state using radiolytically generated $CO_3^{-\bullet}$ radical as a one-electron oxidant. The recovery of the (III,III) state was monitored spectrophotometrically and occurred on a millisecond time scale. The authors claim that water must be the electron donor for this reaction, but do not give proof of dioxygen formation.

It is interesting to note that for both of the above catalysts prepared using the 4,4′- and 5,5′-dicarboxylato-bpy ligand, the active oxidation state is likely to

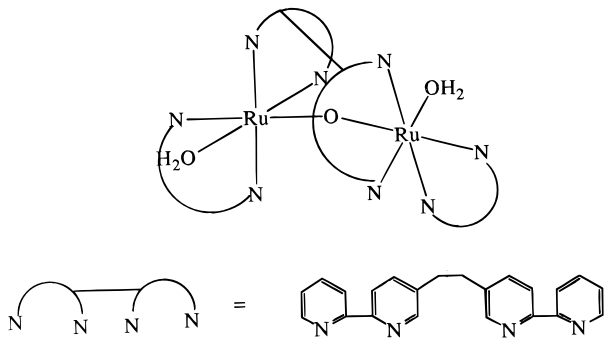

Figure 21. Proposed structure of a Ru dimer with a covalently linked bpy ligand.[16]

be the (IV,IV) state (as compared to (V,V) for (**1**)). First, these complexes are faster catalysts than (**1**) (higher oxidation states cannot be detected in CV experiments), even though their higher oxidation states are less accessible thermodynamically than for (**1**). Of course this comparison is only valid for electrocatalysis experiments and might be influenced by differing electron transfer kinetics of the complexes at the electrodes rather than faster kinetics of the homogeneous reaction steps. Second, the pulse radiolysis studies show that the (IV,IV) state reverts to the (III,III) state (presumably with evolution of O_2) without accumulation of higher oxidation states as intermediates.

Petach and Elliot[16] synthesized sterically constrained Ru-dimers, using covalently linked bpy-x-bpy ligands (Figure 21). Molecular modeling yielded a minimized structure for the dimer in which intramolecular O−O bond formation is excluded by sterical constraints. However, no x-ray structural data exists to support the calculations. The oxo-bridge formed only after electrochemical oxidation beyond the (III,III) state and yielded a mixture of (III,III) and (III,IV) complexes. In aqueous solution only the redox-reaction

$$\text{(III,III)} \xleftrightarrow{1e^-,\ 1H} \text{(III,IV)}$$

could be characterized electrochemically, while catalytic water oxidation interferes above 1.4 V (vs SCE in 0.1 M H_3PO_4). In acetonitrile, however, the (IV,V) oxidation state could be characterized. Electrocatalytic water oxidation occurred at 1.39 V with a Coulombic efficiency of ∼90% (as compared to 13% for (**1**), as reported by Gilbert et al.).

Ramaraj et al. reported the catalytic activity of a number of mono-, di-, and trinuclear Ru complexes.[89,116−118] $[Ru(NH_3)_5(H_2O)]^{3+}$ and $[Ru(NH_3)_6]^{3+}$ oxidize water after Ce(IV) oxidation with turnover numbers of 16 and 8, respectively. It is unclear what the catalytic species really is. The formation of RuO_2 cannot be ruled out. An amide-bridged dimer, $[(NH_3)_5Ru(\mu\text{-}NH_2)_2Ru(NH_3)_5]^{4+}$, absorbed into an ion-exchange resin was also a catalyst. Ru-red and Ru-brown are two commercially available trimers, $[(NH_3)_5RuORu(NH_3)_4ORu(NH_3)_5]^{6+/7+}$, with the Ru oxidation states (III,IV,III) and (IV,III,IV), respectively. According to CV data it was proposed that these complexes can be oxidized to the (V,V,V) oxidation state. The four-electron oxidation of water could therefore be achieved, in principle, with one complex, returning to the (IV,III,IV) state. But this was not established. Turnover numbers as high as 62 were achieved after addition of excess Ce(IV) in aqueous solution.

The oxidation state assignments from cyclic voltammetry of (**1**) by this group are not in accordance with the data by Gilbert et al. (Thus, there is some question about the electrochemical data of all these compounds).

Although (**1**) is not the best catalyst, it remains the most extensively studied one. Mechanisms found for this catalyst, however, do not necessarily apply to similar catalysts (vide supra). For the Ru−ammine complexes, it is doubtful that these species are really the catalytic species, since they are coordinatively saturated and have no substrate (water) bound.

A novel approach to water oxidation/dioxygen evolution using $Ru(bpy)_3^{3+}$ as the catalyst has been adopted by Ledney and Dutta.[17] By synthesizing the catalyst within the 13 Å supercage of zeolite Y, they were able to entrap it and thereby prevent multimetal-centered decomposition reactions that cause catalyst degradation in solution. This proved to be of critical advantage since it allows the slower water-oxidation reaction to dominate. Their mechanism is supported by studies of the intermediates using diffuse reflectance, Raman, EPR, and isotope labeling methods. The principal pathways are summarized in Scheme 4, with selected structures noted in Figure 22.

The favored pathway of reaction occurs under alkaline conditions at pH 12 and results in 70−90% conversion of the oxidizing equivalents stored in the Ru(III) catalyst into dioxygen formation from water. *In situ* catalyst reoxidation with Cl_2 permits multiple cycles of turnover. The first step, eq 1, involves formation of a covalent hydrate at the C4 position of one bpy ligand of the catalyst (Figure 22, species **A**), followed by removal of a proton by hydroxide to form species **B** (eq 2). Intramolecular metal−ligand dismutation (eq 3) is proposed to occur with reduction to Ru(II) and oxidation of the hydroxybipyridyl ligand to the corresponding radical cation, forming species **C**. Slow dissociation of free hydroxyl radical from the coordinated radical cation generating the reduced catalyst is proposed as the rate-limiting step (eq 4). Steps 3 and 4 constitute the thermodynamically demanding steps of this system. In subsequent reactions (eqs 5 and 6), the critical O−O bond-formation step yields hydrogen peroxide. This is proposed to occur in two steps, by initial formation of a biradical species, eq 5, i.e., upon diffusion and addition of the hydroxyl radical to a bipyridyl ligand of a second Ru(III) complex in another supercage, followed by nucleophilic displacement of peroxide upon hydroxide addition to the activated hydroxybipyridyl ligand. In the former species the two oxidizing equivalents formally reside on the ligand and the Ru(III). An alternative pathway (eq 7) can be envisioned for peroxide formation in which hydroxide addition to the Ru(III) complex precedes attack by hydroxyl radical. Subsequent steps (eqs 8 and 9 and 10 and 11) involve pairs of one-electron steps forming superoxide and dioxygen, respectively, using standard chemistry previously documented. The spec-

Scheme 4. Possible Reactions in Water Oxidation by $Ru(bpy)_3^{3+}$ Entrapped in Zeolite[17]

$$Ru(bpy)_3^{3+} + H_2O \longrightarrow \underset{A}{[Ru^{3+}(bpy)_2(bpy\text{-}H_2O)]^{3+}} \quad (1)$$

$$\underset{A}{[Ru^{3+}(bpy)_2(bpy\text{-}H_2O)]^{3+}} + OH^- \longrightarrow \underset{B}{[Ru^{3+}(bpy)_2(bpy\text{-}OH^-)]^{2+}} \quad (2)$$

$$\underset{B}{[Ru^{3+}(bpy)_2(bpy\text{-}OH^-)]^{2+}} \longrightarrow \underset{C}{[Ru^{2+}(bpy)_2(bpy\text{-}OH\cdot)]^{2+}} \quad (3)$$

$$\underset{C}{[Ru^{2+}(bpy)_2(bpy\text{-}OH\cdot)]^{2+}} \longrightarrow Ru(bpy)_3^{2+} + OH^- \quad (4)$$

$$Ru(bpy)_3^{3+} + OH\cdot \longrightarrow [Ru^{3+}(bpy)_2(bpy\text{-}OH\cdot)]^{3+} \quad (5)$$

$$[Ru^{3+}(bpy)_2(bpy\text{-}OH\cdot)]^{3+} + OH^- \longrightarrow Ru(bpy)_3^{2+} + H_2O_2 \quad (6)$$

$$[Ru^{3+}(bpy)_2(bpy\text{-}OH\cdot)]^{3+} + OH\cdot \longrightarrow Ru(bpy)_3^{3+} + H_2O_2 \quad (7)$$

$$Ru(bpy)_3^{3+} + H_2O_2 \longrightarrow Ru(bpy)_3^{2+} + O_2^- + 2H^+ \quad (8)$$

$$Ru(bpy)_3^{3+} + O_2^- \longrightarrow Ru(bpy)_3^{2+} + O_2 \quad (9)$$

$$\underset{B}{[Ru^{3+}(bpy)_2(bpy\text{-}OH^-)]^{2+}} + H_2O_2 \longrightarrow Ru(bpy)_3^{2+} + O_2^- + H_3O^+ \quad (10)$$

$$\underset{B}{[Ru^{3+}(bpy)_2(bpy\text{-}OH^-)]^{2+}} + O_2^- \longrightarrow Ru(bpy)_3^{2+} + O_2 + OH^- \quad (11)$$

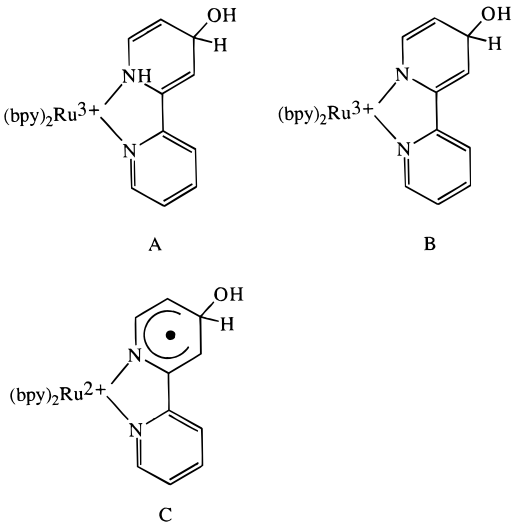

Figure 22. Structures of intermediates in the catalytic water oxidation by $Ru(bpy)_3^{3+}$ entrapped in a zeolite.[17]

troscopic data that are presented are consistent with the presence of the species noted in Scheme 4, but the kinetic data that could test the proposed mechanism are quite limited. The only indication for the involvement of hydroxyl radicals is the detection of the OH adduct with the spin-trap DMPO. However, such an adduct might also be formed after reaction of DMPO with superoxide O_2^- and subsequent decomposition.[119] Hopefully, these deficiencies will be addressed in future studies of this most interesting new system.

X. Nonbiomimetic Water-Oxidation Catalysts

Extensive studies have been done on Ru oxides and other metal oxides as heterogeneous catalysts for water oxidation with either chemical oxidants or in photochemical systems with a photosensitizer and sacrificial electron donor.[120−122] Ru oxides are by now the most efficient and stable water-oxidation catalysts. Silver ions entrapped in zeolite were used in another system capable of oxidizing water.[123] Irradiation of the silver-loaded zeolite leads to photoreduction of the silver ions. The resulting holes are accumulated in the zeolite framework and eventually transferred to water. Another class of catalysts for photooxidation of water are high-bandwidth semiconductors like TiO_2 and ZrO_2. These systems are not discussed here. For further information see, for example, refs 124−127. However, these are heterogeneous catalysts that do not provide mechanistic insights into photosynthetic water oxidation.

On the borderline between heterogeneous and homogenous catalysts lie metal−hydroxo complexes and metal oxide hydrosols with small particle sizes.[128] One study on the mechanism of water oxidation by small Ir oxide clusters is worth mentioning here.[129] Pulse radiolysis and electrochemical studies have been performed on Ir oxide clusters with only four to five Ir atoms per cluster. Such small clusters resemble the core of multinuclear metal complexes with bridging oxo groups and terminal ligands missing. In the case of Ir, it was found that the oxidation state necessary for water oxidation to occur seems to be all-Ir(IV) for the cluster. However, mechanistic details for the O−O bond formation step could not be deduced.

A few other recent systems are also worth mentioning here. Katakis et al.[130,131] formed a system capable of photochemical splitting of water from a tungsten dithiolene complex as the photosensitizer and catalyst with methyl viologen or bipyridinium derivatives as an electron shuttle. The complex (tris-[1-(4-methoxyphenyl)-2-phenyl-1,2-ethylenedithiolenic-

S,S′]tungsten) functioned as the photosensitizer by containing the chromophore for visible light absorption as well as the catalyst for electron and hole transfer to water. It was found that hydrogen and dioxygen evolved in a 2:1 stoichiometry during illumination with light >350 nm in an acetone−water mixture. Using D_2O and acetone-d_6 proved that the hydrogen stems indeed from water reduction. Furthermore, no acetone decomposition product could be detected. When the solution was continuously purged from evolved dioxygen, the catalyst was remarkably stable. Turnover numbers larger than 1000 were achieved without signs of catalyst degradation. The overall light energy storage efficiency was reported as 7%. The simplicity of the system is its most striking feature. However, proof of a mechanism could not be presented.

In another study it was found that trichlorocuprate ions can act similarly as a photocatalyst for water photolysis at very low quantum yield.[132]

XI. Conclusions

The mechanism of water oxidation by the WOC of PSII is still largely unknown. From the physical data available, as well as from the few functioning artificial water oxidation catalysts, a few guidelines for more successful mimics of the WOC can be deduced.

From the theoretical point of view, the concerted four-electron oxidation, which is thermodynamically most feasible, is not necessarily the preferred pathway. It should have a rather high activation barrier because of its high reorganization energy. The fact that there is a variety of related Ru complexes which cannot undergo four-electron reduction, but still oxidize water with higher efficiency than the Ru dimer (that can act as a four-electron acceptor) supports this notion. Furthermore, $[(bpy)_2Ru(O)_2]^{2+}$ can undergo a four-electron reduction with the thermodynamic capability to oxidize water, yet the complex is not functional in this reaction. A pair of dimers is necessary to perform the reaction. The delocalization of the charges and the decreasing reorganization energy for multicenter systems might play a role as well as the existence of an oxo bridge (although there is no evidence for its direct involvement in the mechanism).

Two geometries of model complexes have been used in the two mentioned model cycles of water oxidation for the dioxygen-evolving step by converting oxo bridges to dioxygen. These are the adamantane and cubane structures, described by Wieghardt and Christou (however there is no example of an Mn_4O_4 cubane). These structures are thermodynamically stable and there is no evidence for conversion of oxo groups to H_2O_2 or dioxygen from these structures. Spectroscopy on the WOC suggests that it is rather a distorted nonequilibrium structure with five-coordinate Mn centers that might form a basis for a water-oxidation catalyst. One goal for the future must be to mimic such structures in model complexes.

A. Ru Chemistry

Catalysis of water oxidation by monomeric $[RuL_3]^{3+}$ precursors occurs by inefficient, thermally activated formation of hydroxyl radicals. In the case of L = bpy, the mechanism proceeds by ligand-based hydroxyl radical addition. Thus, in the case of the photosynthetic WOC, the notion of the possible direct involvement of Mn ligands in radical formation at the S_3 state and subsequent catalysis should continue to be explored fully.[50]

For multimeric Ru complexes with terminal and μ-oxos, where intramolecular oxidation of water to peroxide or dioxygen is thermodynamically feasible, the reaction does not appear to be favored kinetically. Thus, there appear to be stereochemical limitations to the intramolecular coupling of oxo ligands in such complexes.

Intermolecular reactions do lead to O_2 formation involving multiple pathways and as-yet unclear chemistry. The involvement of two types of activated oxo groups is implicated: an electrophilic ruthenyl-oxo atom that is tightly bound (slowly exchanging) and a nucleophilic oxo (hydroxo or aquo) anion that is in rapid exchange with solvent water. The catalyst appears to be required to produce both activated species. Mechanistically, this implies that high valent Ru(V) or Ru(IV) may be required for formation of an electrophilic oxo atom, while a lower oxidation state Ru(III) ion in a second catalyst molecule could be envisioned as a Lewis acid needed to bind water and ionize a proton to form a nucleophilic hydroxide substrate. This proposal, although plausible, remains unproven.

B. Mn Chemistry

Much less definitive mechanistic information is available for Mn catalysts. However, the terminal manganoyl(V)-oxo group has emerged as a key precursor to dioxygen formation in porphyrin-based catalysts. These catalysts also showed that, in principle, water oxidation can be achieved at a dinuclear Mn site. As a class, multimeric Mn complexes with bridging oxo ligands do not appear to offer readily accessible oxo ligands for dioxygen formation, but may be further activated to forms of unknown structure.

One common feature of all functioning model systems is their ability to form terminal oxo groups in the highest oxidation state. It seems therefore likely that the formation of the O−O bond can be achieved by solvent attack on terminal oxo groups or inter-/intra-molecular elimination of dioxygen from two such groups. The synthesis of Mn-dimers and higher aggregates with manganoyl groups should be a goal for the future.

XII. Acknowledgments

We thank Drs. R. D. Britt and G. T. Babcock for preprints of their work and Dr. J. Mayer for insightful discussions. The work performed in the authors laboratory has been supported by a grant from the National Institutes of Health (GM39932).

Note Added in Proof

The reactivity of Ar−OH bonds toward H atom abstraction by alkoxyl and peroxyl radicals has been

found experimentally to be considerably faster (10^2−10^4) than C−H bonds of comparable bond dissociation energy, and may, therefore, cast doubt on the transferability of C−H bond kinetic data in the analysis of Mn−OH oxidation kinetics.[133]

XIII. References and Footnotes

(1) DeRose, V. J.; Mukerji, I.; Latimer, M. J.; Yachandra, V. K.; Sauer, K.; Klein, M. P. *J. Am. Chem. Soc.* **1994**, *116*, 5239−5249.
(2) Brudvig, G. W.; Crabtree, R. H., *Proc. Natl. Acad. Sci. U.S.A.* **1986**, *83*, 4586−4588.
(3) Vincent, J. B.; Christou, G., *Inorg. Chim. Acta* **1987**, *136*, L41−L43.
(4) Proserpio, D. M.; Rappe, A. K.; Gorun, S. M., *Inorg. Chim. Acta* **1993**, *213*, 319−324.
(5) Krishtalik, L. I., *Biochim. Biophys. Acta* **1986**, *849*, 162−171.
(6) Knerel'man, E. I.; Luneva, N. P.; Shafirovich, V. Y.; Shilov, A. E., *Kinet. Katal.* **1988**, *29*, 1350−1354.
(7) Lee, D. G.; Moylan, C. R.; Hayashi, T.; Brauman, J. I., *J. Am. Chem. Soc.* **1987**, *109*, 3003−3010.
(8) Boucher, L. J.; Coe, C. G., *Inorg. Chem.* **1975**, *14*, 1289−1295.
(9) Kitajima, N.; Osawa, M.; Tanaka, M.; Moro-oka, Y., *J. Am. Chem. Soc.* **1991**, *113*, 8952−8953.
(10) Matsushita, T.; Fujiwara, M.; Shono, T., *Chem. Lett. (Jpn.)* **1981**, 631−634.
(11) Fujiwara, M.; Matsushita, T.; Shono, T., *Polyhedron* **1985**, *4*, 1895−1900.
(12) Watkinson, M.; Whiting, A.; McAuliffe, C. A., *J. Chem. Soc., Chem. Commun.* **1994**, 2141−2142.
(13) Naruta, Y.; Sasayama, M.; Sasaki, T., *Angew. Chem. Int. Ed. Engl.* **1994**, *33*, 1839−1841.
(14) Kuznetsov, V. L.; Elizarova, G. L.; Matvienko, L. G.; Lantyukova, I. G.; Zhdanov, A.; Shchegolkhina, O. I., *J. Organomet. Chem.* **1994**, *475*, 65−72.
(15) Gilbert, J. A.; Eggleston, D. S.; Murphy, W. R.; Geselowitz, D. A.; Gersten, S. W.; Hodgson, D. J.; Meyer, T. J., *J. Am. Chem. Soc.* **1985**, *107*, 3855−3864.
(16) Petach, H. H.; Elliott, C. M., *J. Electrochem. Soc.* **1992**, *139*, 2217−2221.
(17) Ledney, M.; Dutta, P. K., *J. Am. Chem. Soc.* **1995**, *117*, 7687−7695.
(18) Kalsbeck, W. A.; Thorp, H. H.; Brudvig, G. W., *J. Electroanal. Chem.* **1991**, *314*, 335−343.
(19) Babcock, G. T.; Barry, B. A.; Debus, R. J.; Hoganson, C. W.; Atamian, M.; McIntosh, L.; Sithole, I.; Yocum, C. F. *Biochemistry* **1989**, *28*, 9557−9565.
(20) Baldwin, M.; Gelasco, A.; Pecoraro, V. L., *Photosyn. Res.* **1993**, *38*, 303.
(21) Gardner, K. A.; Mayer, J. A., *Science* **1995**, *269*, 1849−1851.
(22) Krishtalik, L. I., *Biophysics* **1989**, *34*, 958−962.
(23) Hoganson, C. W.; Lydakis-Simantiris, X.; Tang, X.-S.; Tommos, C.; Warnecke, K.; T., B. G.; Diner, B. A.; McCracken, J.; Styring, S., *Photosyn. Res.* **1995**, *46*, 177−184.
(24) Tang, X.-S.; Randall, D. W.; Force, D. A.; Diner, B. A.; Britt, R. D., *J. Am. Chem. Soc.* **1996**, *118*, 7638−7639.
(25) Kleinfeld, D.; Okamura, M. Y.; Feher, G., *Biochim. Biophys. Acta* **1984**, *766*, 126−140.
(26) Pecoraro, V. L.; Baldwin, M. J.; Gelasco, A., *Chem. Rev.* **1994**, *94*, 807−826.
(27) Manchandra, R., Brudvig, G. W.; Crabtree, R. H., *Coord. Chem. Rev.* **1995**, *144*, 1−38.
(28) Debus, R. J., *Biochim. Biophys. Acta* **1992**, *1102*, 269−352.
(29) Sivaraja, M.; Philo, J. S.; Lary, J.; Dismukes, G. C., *J. Am. Chem. Soc.* **1989**, *111*, 3221−3225.
(30) Boussac, A.; Rutherford, A. W., *Biochemistry* **1988**, *27*, 3476−3483.
(31) Dismukes, G. C.; Zheng, M.; Hutchins, R.; Philo, J. S., *Biochem. Soc. Trans.* **1994**, *22*, 323−327.
(32) Joliot, P.; Kok, B. In *Bioenergetics of Photosynthesis*; Govindjee, Ed.; Academic Press: New York, 1975; pp 387−412.
(33) Förster, V.; Junge, W., *Photochem. Photobiol.* **1985**, *41*, 183−190.
(34) Haumann, M.; Junge, W., *Biochem.* **1994**, *33*, 864−872.
(35) Lavergne, J. In *Research in Photosynthesis*; N. Murata, Ed.; Kluwer Academic Publishers: Dordrecht, 1992; Vol. II; pp 273−280.
(36) Babcock, G. T.; Blankenship, R. E.; Sauer, K. *FEBS Lett.* **1976**, *61*, 286−289.
(37) (a) Renger, G.; Weiss, W., *Biochim. Biophys. Acta* **1983**, *850*, 184−196. (b) Dekker, J. P.; Plijter, J. J.; Ouwehand, I., *Biochim. Biophys. Acta* **1984**, *767*, 176−179.
(38) Renger, G.; Hanssum, B., *FEBS Lett.* **1992**, *299*, 28−32.
(39) Liang, W.; Roelofs, T. A.; Olsen, G. T.; Matthew, J. L.; Cinco, R. M.; Rompel, A.; Sauer, K.; Yachandra, V. K.; Klein, M. P. In *Xth International Photosynthesis Congress*; Kluwer Academic Press: Montpellier, France, 1995; pp 413−416.
(40) Messinger, J.; Badger, M.; Wydrzynski, T., *Proc. Natl. Acad. Sci. USA* **1995**, *92*, 3209−3213.
(41) Zimmerman, G., *J. Chem. Phys.* **1955**, *23*, 825−832.
(42) Hillier, W.; Wydrzynski, T., *Photosynth. Res.* **1993**, *38*, 417−424.
(43) Klimov, V. V.; Ananyev, G.; Zastryzhnaya, O.; Wydrynski, T.; Renger, G., *Photosynth. Res.* **1993**, *38*, 409−416.
(44) Fine, P. L.; Frasch, W. D., *Biochemistry* **1992**, *31*, 12204−12210.
(45) Maclachlan, D. J.; Nugent, J. H. A., *Biochemistry* **1993**, *32*, 9772−9780.
(46) Baumgarten, M.; Philo, J. S.; Dismukes, G. C., *Biochemistry* **1990**, *29*, 10814−10822.
(47) Boussac, A.; Zimmermann, J.-L.; Rutherford, A. W., *Biochemistry* **1989**, *28*, 8984−8989.
(48) Sivaraja, M.; Tso, J.; Dismukes, G. C., *Biochemistry* **1989**, *28*, 9459−9464.
(49) Gilchrist, M. L.; Ball, J. A.; Randall, D. W.; Britt, R. D., *Proc. Nat. Acad. Sci. U.S.A.* **1995**, *92*, 9545−9549.
(50) Tommos, C.; Tang, X.-S.; Warnecke, K.; Hoganson, C. W.; Styring, S.; McCracken, J.; Diner, B. A.; Babcock, G. T., *J. Am. Chem. Soc.* **1995**, *117*, 10325−10335.
(51) (a) Mayer, J. M.; Gardner, K. A.; Cook, G. K.; Wang, K.; Adkins, A.; Crevier, T. J.; L., K. L.; Mandel, M. A. In *10th International Symposium on Homogeneous Catalysis*; Princeton, NJ, 1996; pp IL-8. (b) Wang, K.; Mayer, J. M. *J. Am. Chem. Soc.* **1997**, in press.
(52) Bordwell, F. G.; Cheng, J.-P.; Ji, G.-Z.; Satish, A. V.; Zhang, X., *J. Am. Chem. Soc.* **1991**, *113*, 9790−9795.
(53) DeFelippis, M. R.; Murthy, C. P.; Faraggi, M.; Klapper, M. H., *Biochemistry* **1989**, *28*, 4847−4853.
(54) *CRC Handbook of Chemistry and Physics*; Weast, R. C., Astle, M. J., Eds.; CRC Press: Boca Raton, 1982; Vol. 63.
(55) Lind, J.; Shen, X.; Eriksen, T. E.; Merenyi, G. J., *J. Am. Chem. Soc.* **1990**, *112*, 479−482.
(56) Zheng, M.; Dismukes, G. C., *Inorg. Chem.* **1996**, *35*, 3307−3319.
(57) Zheng, M.; Dismukes, G. C. In *Research in Photosynthesis*; Murata, N., Ed.; Kluwer Academic Publ.: Dordrecht, 1992; Vol. II; pp 305−308.
(58) Dismukes, G. C.; Ferris, K.; Watnick, P., *Photobiochem. Photobiophys.* **1982**, *3*, 243−256.
(59) Kusunoki, M.; Ono, T.-A.; Matsushita, T.; Oyanagi, H.; Inoue, Y., *J. Biochem.* **1990**, *108*, 560−567.
(60) Riggs, P. J.; Mei, R.; Yocum, C. F.; Penner-Hahn, J. E., *J. Am. Chem. Soc.* **1992**, *114*, 10650−10651.
(61) Yachandra, V. K.; DeRose, V. J.; Latimer, M. J.; Mukerjee, I.; Sauer, K.; Klein, M. P., *Photochem. Photobiol.* **1991**, *53*, 98−99.
(62) Abragam, A.; Bleaney, B. *Electron Paramagnetic Resonance of Transition Ions*; Oxford University Press: London, **1970**, pp 175.
(63) Liang, W.; Latimer, M. J.; Dau, H.; Roelofs, T. A.; Yachandra, V. K.; Sauer, K.; Klein, M. P., *Biochemistry* **1994**, *33*, 4923−4932.
(64) Penner-Hahn, J. E.; Riggs-Gelasco, P. J.; Yu, E.; DeMarois, P.; Yocum, C. F. In *Xth International Photosynthesis Congress*; Kluwer Academic Press: Montpellier, France, 1995; pp 241−246.
(65) Penner-Hahn, J. E.; Fronko, R. M.; Waldo, G. S.; Yocum, C. F.; Bolby, N. R.; Betts In *Current Research in Photosynthesis*, Kluwer Academic: Netherlands, 1990; Vol. I; pp 797−800.
(66) Volkov, A. G., *Bioelectrochem. Bioenerg.* **1989**, *21*, 3−24.
(67) Brudvig, G. W.; Crabtree, R. H., *Progr. Inorg. Chem.* **1988**, *37*, 99−142.
(68) Wieghardt, K., *Angew. Ch. Int. Ed. Engl.* **1989**, *28*, 1153−1172.
(69) Bashkin, J. S.; Chang, H.-R.; Streib, W. E.; Huffman, J. C.; Hendrickson, D. N.; Christou, G., *J. Am. Chem. Soc.* **1987**, *109*, 6502−6504.
(70) Wang, S.; Tsai, H.-L.; Hagen, K. S.; Hendrickson, D. N.; Christou, G., *J. Am. Chem. Soc.* **1994**, *116*, 8376−8377.
(71) Vincent, J. B.; Christou, G., *Adv. Inorg. Chem.* **1989**, *33*, 197−257.
(72) Wang, S.; Folting, K.; Streib, W. E.; Schmitt, E. A.; McCusker, J. K.; Hendrickson, D. N.; Christou, G., *Angew. Chem. Int. Ed. Engl.* **1991**, *30*, 305−306.
(73) Stibrany, R. T.; Gorun, S. M., *Angew. Ch. Int. Ed. Engl.* **1990**, *29*, 1156−1158.
(74) Proserpio, D. M.; Hoffmann, R.; Dismukes, G. C., *J. Am. Chem. Soc.* **1992**, *114*, 4373−4382.
(75) Krishtalik, L. I., *Biophysics* **1989**, *34*, 1098−1104.
(76) Joliot, P.; Hoffnung, M.; Chabaud, R., *J. Chem. Phys.* **1966**, *63*, 1423−1441.
(77) Sinclair, J.; Arnason, T., *Biochim. Biophys. Acta* **1974**, *368*, 393−400.
(78) Nishida, Y., *Inorg. Chim. Acta* **1988**, *152*, 73−74.
(79) Krishtalik, L. I., *Bioelectrochem. Bioenerg.* **1990**, *23*, 249−263.
(80) Krishtalik, L. I., *J. Mol. Cat.* **1988**, *47*, 211−218.
(81) Shafirovich, V. Y.; Shilov, A. E., *Kinet. Katal. (translated from Russian)* **1979**, *20*, 1156−1162.
(82) Luneva, N. P.; Knerelman, E. I.; Shafirovich, V. Y.; Shilov, A. E., *J. Chem. Soc., Chem. Commun.* **1987**, 1504−1505.

(83) Shafirovich, V. Y.; Shilov, A. E., *Isr. J. Chem.* **1988**, *38*, 149−154.
(84) Luneva, N. P.; Ya., S. V.; Shilov, A. E., *J. Mol. Cat.* **1989**, *52*, 49−62.
(85) Unni Nair, B. C.; Dismukes, C. G., *J. Am. Chem. Soc.* **1983**, *105*, 124.
(86) Elizarova, G. L.; Matvinenko, L. G.; Taran, O. P.; Parmon, V. N.; Kolomiichuk, V. N., *Kinet. Katal. (translated from Russian)* **1992**, *33*, 898−905.
(87) Elizarova, G. L.; Matvienko, L. G.; Pestunova, O. P.; Parmon, V. N., *Kinet. Catal.* **1994**, *35*, 329−333.
(88) Mathews, J. H.; Dewey, L. H., *J. Phys. Chem.* **1913**, *17*, 211−218.
(89) Ramaraj, R.; Kira, A.; Kaneko, M., *Angew. Chem.* **1986**, *98*, 824−825.
(90) Ramaraj, R.; Kira, A.; Kaneko, M., *Chem. Lett.* **1987**, *264*, 261−264.
(91) Yao, G. J.; Kira, A.; Kaneko, M., *J. Chem. Soc., Faraday. Trans. 1* **1988**, *84*, 4451−4456.
(92) Gobi, K. V.; Ramaraj, R.; Kaneko, M., *J. Mol. Cat.* **1993**, *81*, L7−L11.
(93) Otsuji, Y.; Sawada, K.; Morshita, I.; Taniguchi, Y., *Chem. Lett.* **1977**, 983−986.
(94) Thorp, H. H.; Sarneski, J. E.; Brudvig, G. W.; Crabtree, R. H., *J. Am. Chem. Soc.* **1989**, *111*, 9249−9250.
(95) Sarneski, J. E.; Thorp, H. H.; Brudvig, G. W.; Crabtree, R. H.; Schulte, G. K., *J. Am. Chem. Soc.* **1990**, *112*, 7255−7260.
(96) Philouze, C.; Blondin, G.; Girerd, J.-J.; Guilhem, J.; Pascard, C.; Lexa, D., *J. Am. Chem. Soc.* **1994**, *116*, 8557−8565.
(97) Sarneski, J. E.; Brzezinski, L. J.; Anderson, B.; Didiuk, M.; Manchanda, R.; Crabtree, R. H.; Brudvig, G. W.; Schulte, G. K., *Inorg. Chem.* **1993**, *32*, 3265−3269.
(98) Kitajima, N.; Sigh, U. P.; Amagai, H.; Osawa, M.; Moro-oka, Y. *J. Am. Chem. Soc.* **1991**, *113*, 7757−7758.
(99) Mathur, P.; Crowder, M.; Dismukes, G. C., *J. Am. Chem. Soc.* **1987**, *109*, 5227.
(100) Ashmawy, F. M.; McAucliff, C. A.; Parish, R. V.; Tames, J., *J. Chem. Soc., Chem. Commun.* **1984**, 14−16.
(101) Ashmawy, F. M.; McAucliff, C. A.; Parish, R. V.; Tames, J., *J. Chem. Soc, Dalton Trans.* **1985**, 1391−1397.
(102) Aurangzeb, N.; Hulme, C. E.; McAuliffe, C. A.; Pritchard, R. G.; Watkinson, M.; Bermejo, M. R.; Garcia-Deibe, A.; Rey, M.; Sanmartin, J.; Sousa, A., *J. Chem. Soc., Chem. Commun.* **1994**, 1153−1155.
(103) Garcia-Deibe, A.; Sousa, A.; Bermejo, M. R.; Mac Rory, P. P.; McAuliffe, C. A.; Pritchard, R. G.; Helliwell, M., *J. Chem. Soc., Chem. Commun.* **1991**, 728−729.
(104) Meyer, T. J. In *Oxygen Complexes and Oxygen Activation by Transition Metals*; Martell, A. E., Sawyer, D. T.. Eds.; Plenum Press: New York, 1988; pp 33−47.
(105) Gersten, S. W.; Samuels, G. J.; Meyer, T. J., *J. Am. Chem. Soc.* **1982**, *104*, 4029−4030.
(106) Hurst, J. K.; Zhou, J.; Lei, Y., *Inorg. Chem.* **1992**, *31*, 1010−1017.
(107) Ramaraj, R.; Kira, A.; Kaneko, M., *J. Chem. Soc., Faraday Trans. 1* **1986**, *82*, 3515−3524.
(108) Lei, Y.; Hurst, J. K., *Inorg. Chem.* **1994**, *33*, 4460−4467.
(109) Geselowitz, D.; Meyer, T. J., *Inorg. Chem.* **1990**, *29*, 3894−3896.
(110) Doppelt, P.; Meyer, T. J., *Inorg. Chem.* **1987**, *26*, 2027−2034.
(111) Raven, S. J.; Meyer, T. J., *Inorg. Chem.* **1988**, *27*, 4478−4483.
(112) Lei, Y.; Hurst, J. K., *Inorg. Chim. Acta* **1994**, *226*, 179−185.
(113) Rotzinger, F. P.; Munavalli, S.; Comte, P.; Hurst, J. K.; Gratzel, M.; Pern, F.-J.; Frank, A. J., *J. Am. Chem. Soc.* **1987**, *109*, 6619−6626.
(114) Nazeeruddin, M. K.; Rotzinger, F. P.; Comte, P.; Gratzel, M., *J. Chem. Soc., Chem. Commun.* **1988**, 872−874.
(115) Comte, P.; Nazeeruddin, M. K.; Rotzinger, F. P.; Frank, A. J.; Gratzel, M., *J. Mol. Catal.* **1989**, *52*, 63−84.
(116) Ramaraj, R.; Kira, A.; Kaneko, M., *J. Chem. Soc., Chem. Commun.* **1986**, 1707−1709.
(117) Ramaraj, R.; Kira, A.; Kaneko, M., *J. Chem. Soc., Chem. Commun.* **1987**, 227−228.
(118) Ramaraj, R.; Kaneko, M.; Kira, A., *Bull. Chem. Soc. Jpn.* **1991**, *64*, 1028−1030.
(119) (a) Dikalov, S. I.; Kirilyuk, I. A.; Grigor'ev, I. A.; Volodarskii, L. B., Translated from *Izvestia Akademii Nauk (Bull. Russ. Acad. Sci.)* **1992**, 1064−1068. (b) Britigan, B. E.; Rosen, G. M.; Chai, Y., Chohen, M. S. *J. Biol. Chem.* **1986**, *261*, 4426−4431.
(120) Mills, A., *Chem. Soc. Rev.* **1989**, *18*, 285−316.
(121) Harriman, A.; Pickering, I. J.; Thomas, J. M., *J. Chem. Soc., Faraday Trans. 1* **1988**, *84*, 2795−2806.
(122) Mills, A.; Davies, H. L., *Electrochim. Acta* **1992**, *37*, 1217−1225.
(123) Beer, R.; Calzaferri, G.; Li, J.; Waldeck, B., *Coord. Chem. Rev.* **1991**, *111*, 193−200.
(124) Norton, A. P.; Bernasek, S. L.; Bocarsly, A. B., *J. Phys. Chem.* **1988**, *92*, 6009−6016.
(125) Tennakone, K.; Tantrigoda, R.; Abeysinghe, S.; Punchihewa, S.; Fernando, C. A. N., *J. Photochem. Photobiol. A* **1990**, *52*, 43−46.
(126) Salvador, P.; Gonzalez, M. L. G., *J. Phys. Chem.* **1992**, *96*, 10349−10353.
(127) Sayama, K.; Arakawa, H., *J. Phys. Chem.* **1993**, *97*, 531−533.
(128) Nahor, G. S.; Mosseri, S.; Neta, P.; Harriman, A., *J. Phys. Chem.* **1988**, *92*, 4499−4504.
(129) Nahor, G. S.; Hapiot, P.; Neta, P.; Harriman, A., *J. Phys. Chem.* **1991**, *95*, 616−621.
(130) Katakis, D. F.; Mitsopoulou, C.; Konstantatos, J.; Vrachnou, E.; Falaras, P., *J. Photochem. Photobiol.* **1992**, *68*, 375−388.
(131) Katakis, D.; Mitsopoulou, C.; Vrachnou, E., *J. Photochem. Photobiol.* **1994**, *81*, 103−106.
(132) Tennakone, K.; Punchiheva, S.; Jayasuriya, A. C.; Perera, W. A. C., *J. Photochem. Photobiol. A* **1990**, *52*, 281−284.
(133) Foti, M.; Ingold, K. U.; Lusztyk, J. *J. Am. Chem. Soc.* **1994**, *116*, 9440−9447.

CR950201Z